Master's Thesis

Cellular distribution and amounts of positive and negative RNA strands of enterovirus during an infection *in vitro*

Sami Salmikangas

University of Jyväskylä

Department of Biological and Environmental Science

Cellular and Molecular Biology

5.5.2020

UNIVERSITY OF JYVÄSKYLÄ, Faculty of Mathematics and Science
Department of Biological and Environmental Science
Cellular and Molecular Biology

Sami Salmikangas: Cellular distribution and amounts of positive and negative RNA strands of enterovirus during an infection *in vitro*

MSc thesis: 36 p., 1 appendix (6 p.)
Supervisors: Docent Varpu Marjomäki
May 2020

Keywords: Amplification, antiviral drugs, branched DNA, confocal microscopy, fluorescence, in-situ hybridization, replication, RNA

Enteroviruses are small, non-enveloped viruses with a positive-sense RNA genome. Over a hundred different serotypes of enteroviruses can infect humans, and they can cause a wide range of diseases from common colds to encephalitis and myocarditis. The life cycle of enteroviruses is relatively well known, but the distribution of the positive RNA genome and its complementary negative RNA strands during an infection are unknown, mostly due to lacking techniques. Certain antiviral drugs could target this step of the life cycle, inhibiting the synthesis of the negative strand and stopping the infection, but to study this in more detail, new methods are required to visualise the viral RNAs effectively. In this study, we developed a protocol to study the enterovirus RNAs using branched DNA fluorescence in-situ hybridization. With this method, along with reverse transcription quantitative PCR, we studied the distribution and the amounts of enterovirus RNAs during an infection *in vitro*. The results indicate that the amounts of positive-, negative- and double stranded RNAs are negligible before 3 hours post-infection, and gradually rise after 4-5 hours post-infection. The positive RNA is located peripherally in the cell with the negative RNA and double stranded RNA being located more centrally. Furthermore, the RNA molecules reside in different locations than the viral capsid proteins and the cell nuclei. We also tested the effect of three different antiviral drugs on the distribution and amounts of viral RNAs, and the results show that all tested molecules effectively inhibit the infection and the appearance of viral RNAs. These results, along with the branched DNA protocol we established, will be useful in more efficiently studying the life cycle of enteroviruses and in the development of antiviral drugs.

JYVÄSKYLÄN YLIOPISTO, Matemaattis-luonnontieteellinen tiedekunta
Bio- ja ympäristötieteiden laitos
Solu- ja Molekyylibiologia

Sami Salmikangas: Enteroviruksen positiivisten ja negatiivisten RNA juosteiden jakauma ja määrä solussa infektion aikana
Pro gradu -tutkielma: 36 s., 1 liite (6 s.)
Työn ohjaajat: Dosentti Varpu Marjomäki
Toukokuu 2020

Hakusanat: Amplifikaatio, branched DNA, fluoresenssi, in-situ hybridisaatio, konfokaalimikroskopia, replikaatio, RNA, viruslääkkeet

Enterovirukset ovat pieniä vaipattomia viruksia, joilla on positiivinen RNA-genomi. Ihmisille infektiivisiä enteroviruksia tunnetaan yli sata erilaista, ja ne voivat aiheuttaa monia tauteja normaalista flunssasta sydänlihastulehdukseen ja aivokalvontulehdukseen. Enterovirusten elämänkierto tunnetaan melko hyvin, mutta riittämättömien menetelmien takia niiden positiivisen RNA-genomin sekä negatiivisten RNA-juosteiden jakaumaa ja määrää solussa infektion aikana ei tunneta juurikaan. Viruslääkkeitä voitaisiin suunnitella estämään mitä tahansa viruksen elämänkierron vaihetta, mutta tätä varten tarvitaan uusia tekniikoita tutkia RNA-juosteita infektion aikana. Tässä tutkimuksessa kehitimme branched DNA in-situ fluoresenssi hybridisaatioon perustuvan uuden protokollan, ja käytimme tätä metodia käänteistranskriptio – kvantitatiivisen PCR:n ohella enterovirusten RNA-juosteiden jakauman ja määrän tutkimiseen infektion aikana. Tulostemme mukaan viruksen positiivisen-, negatiivisen- sekä kaksoisjuosteisen RNA:n määrä on lähes olematon ennen kolmea tuntia infektion jälkeen, ja niiden määrä kasvaa huomattavasti 4-5 tuntiin infektion jälkeen. Positiivinen RNA on jakautunut solun ulkoreunoille, kun taas negatiivinen ja kaksoisjuosteinen RNA on lähempänä solun tumaa. RNA juosteet eivät lokalisoidu viruksen kapsidin tai solun tuman kanssa. Testasimme myös kolmen eri viruslääkkeen vaikutusta RNA-juosteiden määrään ja jakaumaan solussa, ja tulostemme mukaan kaikki lääkkeet estivät virusinfektion ja viruksen RNA-synteesin lähes kokonaan. Nämä tulokset, kehittämämme protokollan ohella, auttavat tutkimaan enterovirusten elämänkiertoa tehokkaammin ja kehittämään uusia mahdollisia viruslääkkeitä.

TABLE OF CONTENTS

TERMS AND ABBREVIATIONS

CVB3	Coxsackie virus B 3
CVA9	Coxsackie virus A 9
EV1	Echovirus 1
RO	Replication organelle
VP	Viral capsid protein
+RNA	Positive sense RNA genome of enteroviruses
-RNA	Negative sense complementary RNA
dsRNA	Double stranded RNA
FISH	Fluorescence in-situ hybridization
bDNA-FISH	Branched-DNA fluorescence in-situ hybridization
RT-qPCR	Reverse transcription quantitative real-time polymerase chain reaction
Cq-value	Quantitation cycles in qPCR
Rac1-I	Rac1 inhibitor
Cal-I1	Calpain inhibitor 1
IHD	Unpublished in-house antiviral drug
p.i.	Post-infection
DMEM	Dulbecco's modified eagle medium
FBS	Fetal bovine serum
PFA	Paraformaldehyde
BSA	Bovine serum albumin
PBS	Phosphate buffered saline

1 INTRODUCTION

1.1 Classification and epidemiology of enteroviruses

The genus *Enterovirus* belongs to the family of *Picornaviridae*, and Enteroviruses are classified into 13 species (Baggen *et al.* 2018). Over a hundred different enterovirus serotypes can infect humans, and they all belong to the species Enterovirus A-D or Rhinovirus A-C according to their molecular and/or antigenic characteristics. Enteroviruses include for example coxsackie viruses, polioviruses, rhinoviruses and echoviruses, and the enterovirus species B contains 63 different serotypes of coxsackie- and echoviruses. These include the viruses in focus of this study, which are coxsackie virus B 3 (CVB3), coxsackie virus A 9 (CVA9) and echovirus 1 (EV1).

Enteroviruses can cause a range of diseases from minor common colds and rashes to severe conditions such as myocarditis, meningitis and encephalitis (Pons-Salort *et al.* 2015). Some chronic diseases, such as atherosclerosis and type 1 diabetes, have also been linked to enteroviruses (Hober and Sauter 2010; Roivainen *et al.* 1998). Enterovirus vaccines have only been developed against poliovirus and enterovirus 71, despite the prevalence of diseases caused by enteroviruses. Some antiviral drugs have been, or are being developed, against enteroviruses, but none have made it to commercial markets yet.

1.2 Structure and life cycle of enteroviruses

Enteroviruses are small (~30 nm), non-enveloped RNA viruses and they have high mutation and recombination rates (Tuthill *et al.* 2010). They have icosahedral capsids with 2-, 3- and 5- fold symmetries (Figure 1a), and the capsid consists of 60 repeating protomers which are made from the viral capsid proteins VP1, VP2, VP3 and VP4 (Figure 1c). The VP4 protein is located mostly inside the capsid, whereas the surface of the capsid is composed of the proteins VP1, VP2 and VP3 (Figure 1b). Most enterovirus capsids also have large ~12 Å deep and ~15 Å wide canyons surrounding each fivefold axis (Figure 1a), hiding some highly conserved amino

acid residues used as receptor binding sites (Rossmann *et al.* 2002). Inside the capsid, enteroviruses have a single stranded positive-sense RNA genome (+RNA).

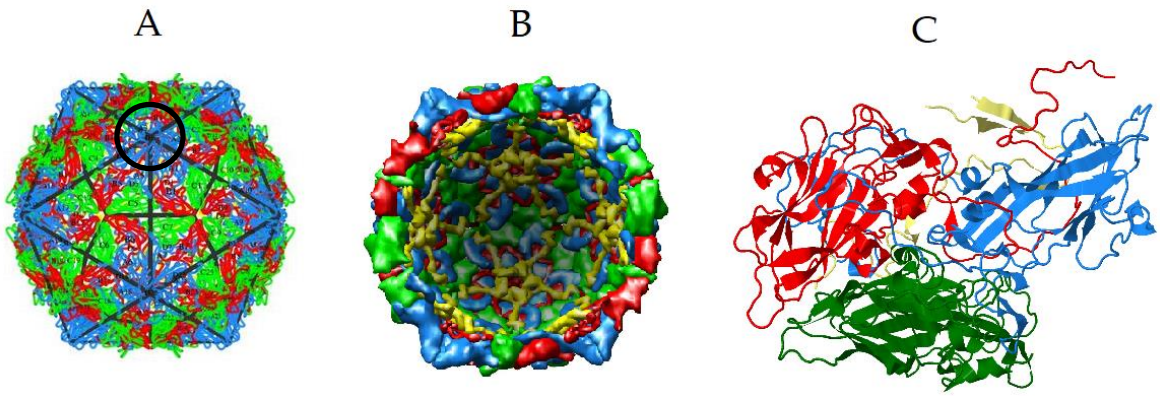

Figure 1. Representation of the capsid of CVB3. (a) The capsid of an enterovirus is icosahedral, and the 2-, 3- and 5-fold symmetries of the capsid are marked with black lines. VP1 is blue, VP2 is red and VP3 is green. The canyon is marked with a black circle. **(b)** The inside view of the capsid shows the VP4 capsid protein, coloured yellow in the image. **(c)** Ribbon presentations of the viral capsid proteins VP1-VP4. The images were acquired using the 3D viewer in ViperDB (http://viperdb.scripps.edu/) PDB ID: 1COV.

The life cycle of enteroviruses starts with attachment, where the virus binds to the cells surface receptor(s) (Figure 2) (Baggen *et al*. 2018). The binding causes receptor-mediated endocytosis of the virus particle by the cell, after which a change in pH (endosome maturing), receptor binding or ionic changes (Ruokolainen et al. 2019) will lead to uncoating of the virus. During uncoating, the viral genome is first released from the capsid into the endosome, and then through the endosomal membrane and into the cytosol. In the cytosol, the +RNA is translated, resulting in a single polyprotein, which is subsequentially cleaved by viral proteases $2A^{pro}$, $3C^{pro}$ and $3CD^{pro}$ into capsid proteins VP0 (intermediate polyprotein for VP2 and VP4), VP1 and VP3 and replication proteins 2A-2C and 3A-3D. The viral genome replication is started by the RNA polymerase $3D^{pol}$ - protein, which synthesizes a negative RNA strand (-RNA) to serve as a template for new +RNA strands. The -RNA and +RNA strands form both stable and unstable double stranded RNA (dsRNA) intermediates as well. The new +RNA strands are then used to generate new -RNA strands, translated to create more capsid proteins, and/or assembled into new provirions with the capsid protein pentamers. The pentamers are created by combining five capsid protomers, which include the VP0, VP1 and VP3 capsid proteins, into a pentamer (Baggen *et al*. 2018).

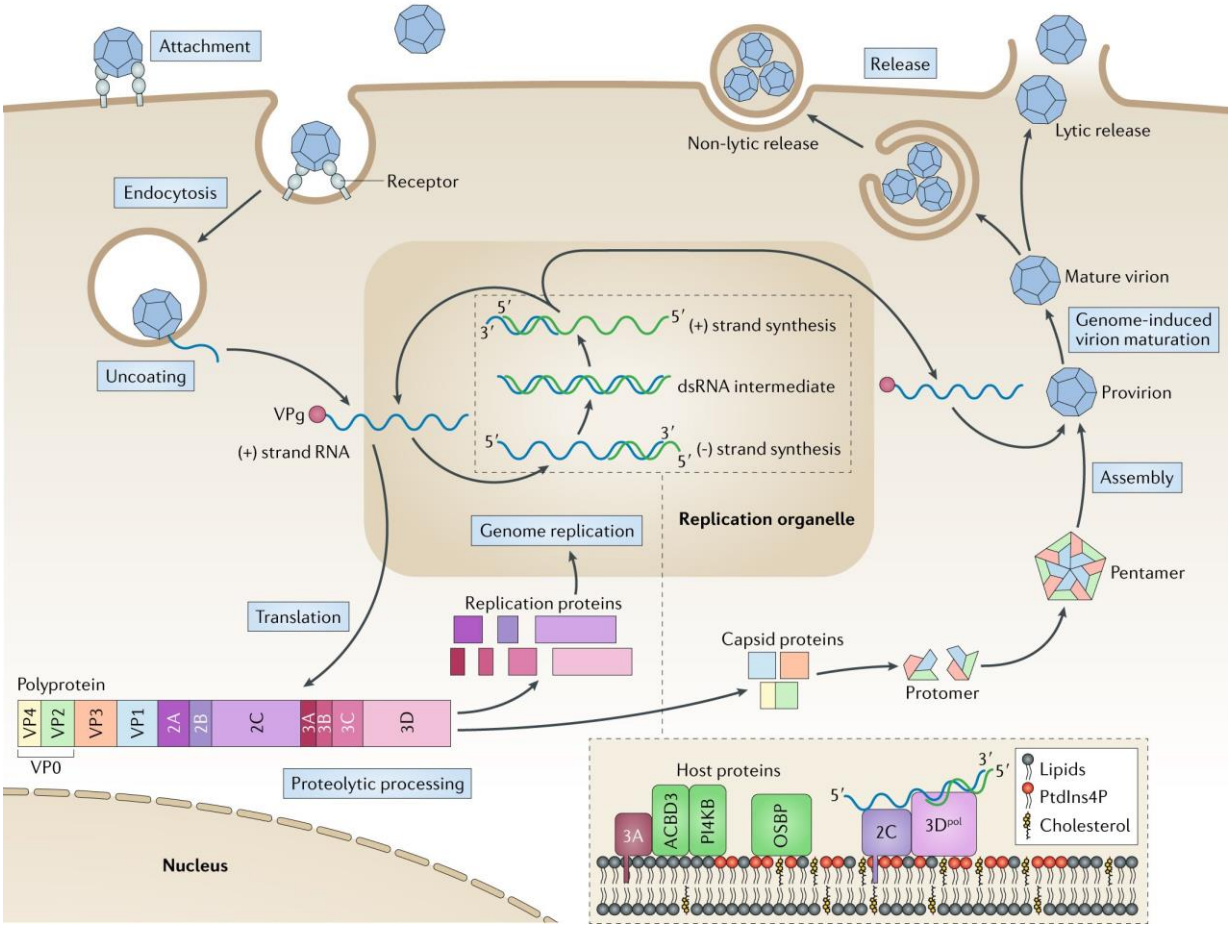

Figure 2. An overview of the life cycle of an enterovirus. Figure modified from the article by Baggen et al. 2018, figure 2. Copyright: Springer Nature, reproduced with permission.

The genome replication of the virus takes place in replication organelles (ROs), which are intracellular membranes rearranged and repurposed by the virus to serve as a factory for genome replication (van der Schaar *et al*. 2016). ROs gather viral- and host proteins into themselves to mediate efficient replication and to protect the viruses from cellular RNAases and antiviral-response-triggering proteins. ROs' structures change during the course of the infection depending on the needs of the virus, from single-membrane tubules to double-membrane vesicles and on to multilamellar structures. ROs are constructed by the viral proteins 2B, 2C and 3A, together with host proteins acyl-CoA-binding domain-containing protein (ACBD3), phosphatidylinositol 4-kinase-β (PI4KB) and oxysterol-binding protein (OSBP) (van der Schaar *et al*. 2016).

After assembling the viral +RNA and translated and cleaved capsid proteins VP0, VP1 and VP3 into a provirion, the RNA induces the cleavage of VP0 into VP2 and

VP4, resulting in a mature and infective virus particle (Basavappa *et al.* 1994). Some of the pathways and mechanisms underlying in how the virus induces cell lysis are still unclear. What we do know, is that viral proteases $2A^{pro}$ and $3C^{pro}$ induce host shut-off, interrupt interferon- and stress pathways and disrupt the cytoskeleton and nucleocytoplasmic transport, ultimately leading to cell lysis (Harris and Coyne, 2014). Newly synthesized, mature and infective viruses are released during the cell lysis into the surrounding extra-cellular matrix and make their way to infect new cells. In recent studies it has been shown that some enteroviruses are also capable of leaving the cell in extracellular vesicles in a non-lytic fashion (Lai *et al.* 2016). The genome replication and translation are highly conserved between different enterovirus species, making these steps ideal targets for antiviral drugs (Baggen *et al.* 2018). Many enterovirus inhibitors have been/are being tested, but there is still a great need for efficient and non-toxic antiviral drugs.

1.3 Branched DNA FISH

The current methods and technology to study the distribution and dynamics of viral RNA molecules inside an infected cell are not ideal, as electron microscopy and immunohistochemistry can only detect mature virions, and quantitative real-time PCR (qPCR) is not suited to study the distribution and dynamics of RNAs. Fluorescence in-situ hybridization (FISH) techniques try to remedy this situation but are limited by low signal intensity and nonspecific probe binding. Branched DNA FISH (bDNA FISH) based methods can detect single RNA molecules with confocal microscopy and is our choice of method for studying the distribution of enterovirus RNA molecules during an infection *in vitro* in this study.

The bDNA FISH technology, originally developed by Affymetrix (now Thermo Fisher), relies on hybridizing tiers of DNA oligos on top of a target RNA probe (Battich et al., 2013). The preamplifier and amplifier DNA oligos create a "branched tree" type of DNA structure, where up to 8000 fluorophore-conjugated label probes can then be hybridized to (Figure 3). This is sufficient to detect even single RNA molecules with a confocal microscope, whereas traditional, non-amplified FISH

techniques require a 600-times longer exposure and a 100-times greater camera gain than bDNA FISH to be able to see similar discernible spots (Battich et al., 2013). This technique can also be coupled with standard antibody-based immunofluorescence to detect for example viral capsid proteins. We decided to use the ViewRNA® Cell Plus Assay Kit by Thermo Scientific for our bDNA FISH experiments. The available fluorophores for ViewRNA are Alexa Fluor® 488, Alexa Fluor® 546 and Alexa Fluor® 647.

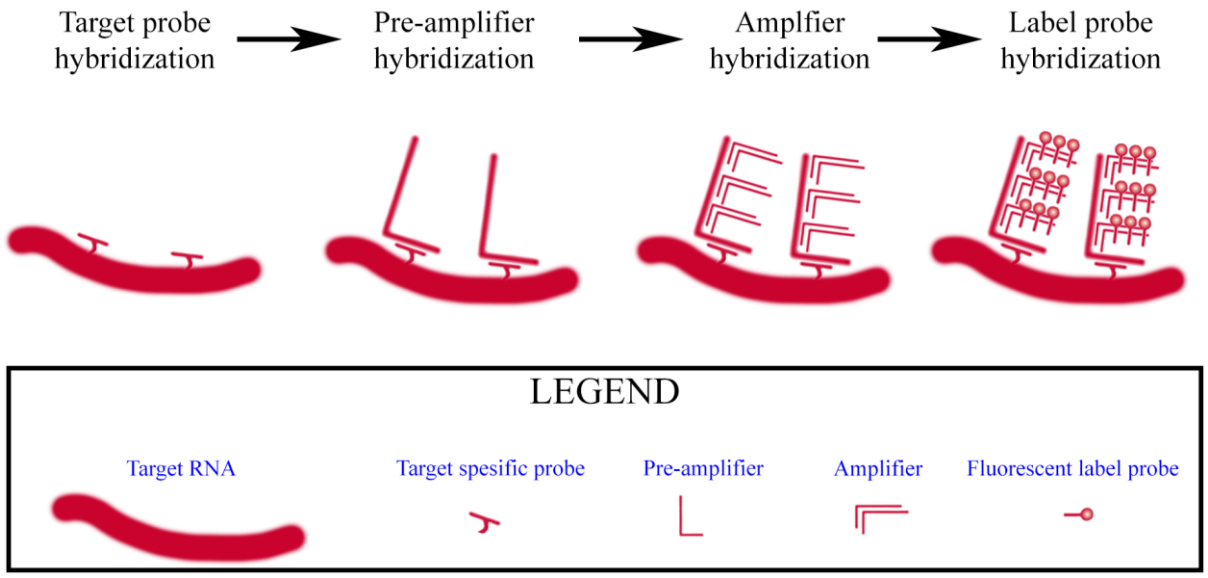

Figure 3. bDNA FISH technology overview. Probe set(s) designed for the target RNA(s) are first hybridized to the target RNA(s). Then a set of preamplifier DNA oligos are hybridized to the probe, followed by amplifier DNA oligos. This creates a "branched tree" of DNA oligos, where thousands of fluorescent label probes can then be hybridized to, to amplify the target RNA signal.

The bDNA FISH technology and the ViewRNA kit have been successfully used before to detect both positive- and negative sense viral RNAs (e.g. Zhang *et al.*, 2017; van Buuren and Kirkekaard, 2018), but to our knowledge, bDNA FISH has never been used to detect enterovirus RNA. Since enteroviruses generate only small amounts of -RNA, about 40- to 100-fold less than +RNA (Novak and Kirkekaard, 1991), and the RNA strands form double stranded RNA intermediates, the -RNA can be difficult to detect with FISH techniques. In this study, we set out to establish a protocol to detect both negative- and positive sense enterovirus RNA molecules during an infection *in vitro* using bDNA FISH and confocal microscopy, and to

study the cellular distribution and dynamics of said RNA molecules during an enterovirus infection.

1.4 RT-qPCR

Reverse transcription quantitative real-time polymerase chain reaction (RT-qPCR) analysis is a very sensitive and reliable method for nucleic acid concentration measurements (Kralik and Ricchi, 2017). In RT-qPCR, the RNA is extracted from the cells, converted to complementary DNA (cDNA) by a reverse transcriptase enzyme and amplified with a qPCR reaction. In the qPCR reaction, the SYBR green dye binds to double stranded DNA and emits low fluorescence when unbound and high fluorescence when bound, effectively doubling the total fluorescence with every PCR cycle (Figure 4).

The data from RT-qPCR comes in the form of quantitation cycles (Cq), which means the amount of PCR cycles it takes for the total fluorescence to cross a certain threshold. The threshold is set so that the fluorescence of the PCR product can be detected above the background signal, and the threshold is the same for all samples. The higher the Cq value is, the lower the amount of initial template there is in the sample. It is noteworthy that Cq values provide no absolute quantification of the initial template amount; the results are comparable only between each other inside each study.

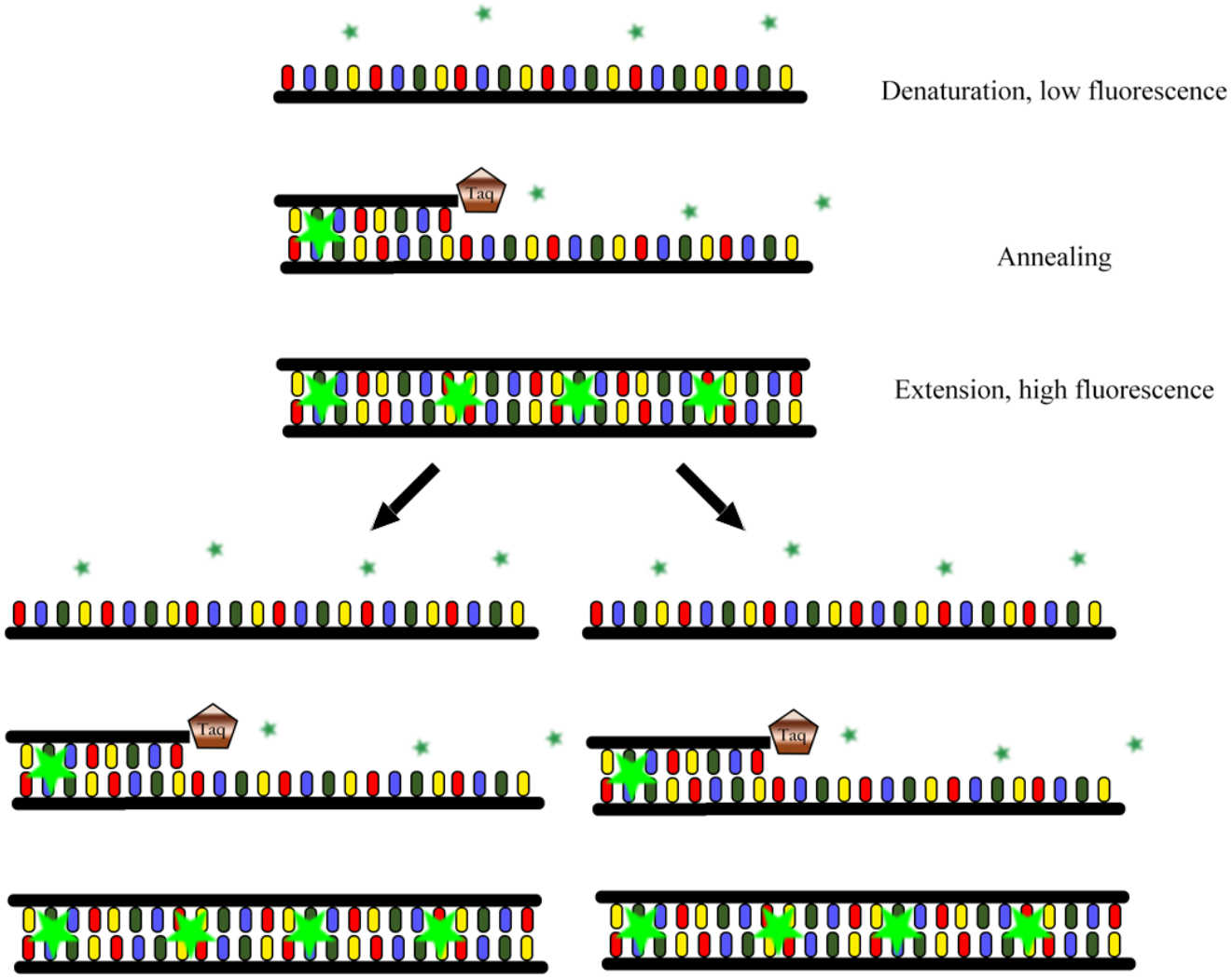

Figure 4. Illustrative figure of a qPCR reaction. The template strand is first denatured, and little to no dye is bound to the single DNA strands. After the temperature is raised, primers anneal to the strands and the polymerase enzyme starts constructing a new strand from free nucleotides based on the template. After the extension is complete, the dye binds to the double stranded DNA and emits fluorescent light, which is read by the qPCR machine.

1.5 Antiviral drugs and their targets

Along with vaccines, antiviral drugs have shown great promise in the treatment of diseases caused by viruses, as each step of the virus replication cycle can be targeted (Lin et al., 2019). As of yet, there are no vaccines or antiviral drugs against non-polio enteroviruses on the market, with the exception of a promising inactivated Enterovirus 71 vaccine in China (Head et al., 2019). In this study, we decided to test the effect of three different drugs on the amount and distribution of enterovirus +RNA and -RNA molecules during an infection *in vitro*. The drugs used are Rac1 inhibitor NSC23766 (Rac1-I), Calpain inhibitor 1 (Cal-I1) and an unpublished in-

house antiviral drug (IHD), and they have previously been shown to have antiviral activity (Upla et al., 2008; Huttunen et al., 2014). These antivirals target cellular proteins that are essential for the virus replication cycle, since targeting the host factors instead of the virus particles themselves creates a higher barrier for the virus to develop drug resistances (Lin & Gallay, 2013).

Rac1 is a small cellular Rho GTPase protein that regulates the amount and distribution of guanosine triphosphate (GTP), an important cellular signalling molecule, by hydrolysing it to guanosine diphosphate (GDP) (Etienne-Manneville and Hall, 2002). By modifying the actin cytoskeleton, GTPases regulate many cellular processes, such as motility, gene expression and cell cycle, but have also important supportive and suppressive functions in viral life cycles (Dierkes et al., 2014). It has been shown that Rac1 is involved in the regulation of the entry of enteroviruses into the cell (Karjalainen et al., 2008), and thus is an important host factor in enterovirus infections. The Rac1 inhibitor NSC23766 specifically inhibits Rac1 without effecting other proteins of the Rho GTPase family (Gao et al., 2004), making it an ideal candidate for an antiviral drug.

Calpains are calcium-dependent cysteine proteases expressed in all mammals (Ono and Sorimachi, 2012). Their normal role in the cell is to catalyse the processing of cytoplasmic proteins, but they have a role in the replication cycle of enteroviruses as well (Upla et al., 2008; Bozym et al., 2010). Unlike the Rac1 protein described above, calpains 1 and 2 are not required for the entry of the virus, but rather at later stages of the infection in RNA replication (Upla et al., 2008). It was recently demonstrated that cellular calpains can cleave viral capsid proteins VP1 and VP3 from the enterovirus polyprotein (Laajala et al., 2019), and that enterovirus infection upregulates the activity of calpains, suggesting that calpains are essential for the cleavage of the viral polyprotein. Laajala et al. also demonstrated high cross-reactivity of calpain inhibitor 1 with the viral proteases $2A^{pro}$ and $3C^{pro}$, making it a promising antiviral drug.

Properties and targets of the in-house drug are not described here as that is still unpublished data.

1.6 Aims of the study

The distribution and amounts of enterovirus RNAs during an infection are quite unknown to this date, mostly due to lacking techniques to study them. This is particularly true for the rare -RNA strands, since the amount of -RNA during the course of an enterovirus infection is very limited, making it even harder to detect. Studying the distribution and amounts of enterovirus RNAs (both + and -) during an infection with bDNA FISH and RT-qPCR can give valuable information about the infection itself, about how to target the viral life cycle and can help to develop novel methods to study enterovirus RNAs and infections.

The research questions of this study are:

1. Is bDNA-FISH a suitable method to detect the +RNA and -RNA strands of an enterovirus, and can it be used to study the distribution of these RNA molecules during an enterovirus infection *in vitro*?
2. What are the amounts of enterovirus +RNA and -RNA strands in an infected cell and how do the amounts change during an infection?
3. Is the synthesis of the +RNA and/or -RNA strands inhibited by Rac1-I, Cal-I1 and/or IHD?

The aims of this study are:

1. To develop a bDNA-FISH based protocol that is able to detect individual intracellular enterovirus +RNA and -RNA strands with confocal microscopy
2. To characterize the distribution, dynamics and amounts of the enterovirus RNAs during an infection
3. To study if the synthesis of enterovirus -RNA and/or +RNA strands are inhibited by Rac1-I, Cal-I1 and/or IHD.

2 MATERIALS AND METHODS

2.1 Cell culturing

Human alveolar basal epithelial A549 cells (ATCC) were used in the experiments and cultivated in 37 °C in Dulbecco's Modified Eagle's Medium (DMEM, Gibco Life Technologies, Ref. 52100-039) supplemented with 10% Fetal Bovine Serum (FBS, Gibco Life Technologies, Ref. 10270-106), 1% L-Glutamine (Gibco Life Technologies, Ref. 35050-038) and 1% penicillin and streptomycin (Gibco Life Technologies, Ref. 15130-122). The cells were sub-cultured 1:10 – 1:20 every few days to keep the cells sub-confluent. Whenever needed in the experiments, the cells were sub-cultured and cultivated in 5 ml dishes (21.5 cm^2) on round coverslips.

2.2 Virus infections

Coverslips 70-80% confluent with cells were transferred to sterile 4-well plates (Thermo Scientific, Ref. 176740) and infected with in-house purified CVA9 virus (Griggs strain, infectivity 1.6 x 10^{11}), CVB3 virus (Nancy strain, infectivity 1.1 x 10^{12}) or EV1 virus (Farouk strain, infectivity 1.1 x 10^{12}) by diluting the virus 1:3000 in DMEM supplemented with 1% FBS. Viruses were allowed to bind to the cells for 45 minutes on ice, following a wash with cold 0.5% bovine serum albumin (BSA) in phosphate buffered saline (PBS) before starting the infection to ensure an even infection rate. The infection was started by changing the media to DMEM supplemented with 10% FBS and incubating the cells at 37 °C for 1-6 hours, depending on the experiment. The infected cells were then fixed with the ViewRNA Cell Plus Assay kit's (Invitrogen, Ref. 88-19000-99) fixation/permeabilization solution for 30 minutes at room temperature (RT). For the immunofluorescence assays without the ViewRNA kit, the cells were fixed with 4% paraformaldehyde in PBS (thawed from in-house frozen stocks, originally prepared from paraformaldehyde, Sigma Aldrich, Ref. P6148) for 30 minutes at RT and permeabilized with 0.2% Triton X-100 (ICN Biomedicals Inc., Ref. 194854) for 5 minutes at RT.

2.3 Immunofluoresence

Immunofluorescence was performed with either commercial or in-house primary antibodies and commercial fluorescent secondary antibodies (Table 1). Immunofluorescence with the ViewRNA kit was performed by incubating the cells first in the kit's Antibody Diluent/Blocking Solution for 20 minutes at RT, then in primary antibody diluted in the kit's Antibody Diluent/Blocking Solution for 1 hour at RT and finally in secondary antibody diluted in the kit's Antibody Diluent/Blocking Solution for 30 minutes at RT. The cells were washed 3 times with the kit's 1x PBS with RNase Inhibitors between each incubation.

Table 1. Antibodies used in the immunofluorescence and bDNA FISH.

Antibody	**Primary/Secondary**	**Final concentration**	**Origin**
CVA9-8863 rabbit monoclonal antibody	Primary (rabbit anti-CVA9 capsid)	1:100	Merja Roivainen, THL, Helsinki
CVA9-861 rabbit monoclonal antibody	Primary (rabbit anti-CVA9 capsid)	1:100	Merja Roivainen, THL, Helsinki
CVA9-K3 rabbit monoclonal antibody	Primary (rabbit anti-CVA9 capsid)	1:100	Merja Roivainen, THL, Helsinki
J-2 mouse mono-clonal antibody	Primary (mouse anti-dsRNA)	1:8000	Scicons (Prod.No. 10010200)
Goat anti-Rabbit IgG (H+L) Secondary Antibody, Alexa Fluor 488 (GAR488)	Secondary (goat anti-rabbit)	1:400	Invitrogen/ Molecular Probes, Ref. A-11008
Goat anti-Mouse IgG (H+L) Secondary Antibody, Alexa Fluor 488 (GAM488)	Secondary (goat anti-mouse)	1:400	Invitrogen/ Molecular Probes, Ref. A-11029
Goat anti-Mouse IgG (H+L) Secondary Antibody, Alexa Fluor 633 (GAM633)	Secondary (goat anti-mouse)	1:400	Invitrogen/ Molecular Probes, Ref. A-21052

2.4 bDNA FISH

bDNA FISH with the ViewRNA assay kit was performed according to the manufacturer's instructions, with the exception of a 15-minute incubation with 95% formamide in 0.1% SSC buffer at 65 °C before the addition of the primary RNA probes. Workflow for the bDNA FISH is detailed in figure 5. The primary RNA probes (EVAB- for -RNA and EVAB+ for +RNA) were kindly provided by Heikki Hyöty's group (University of Tampere). A detailed protocol for performing the bDNA FISH experiment is provided in Appendix 1.

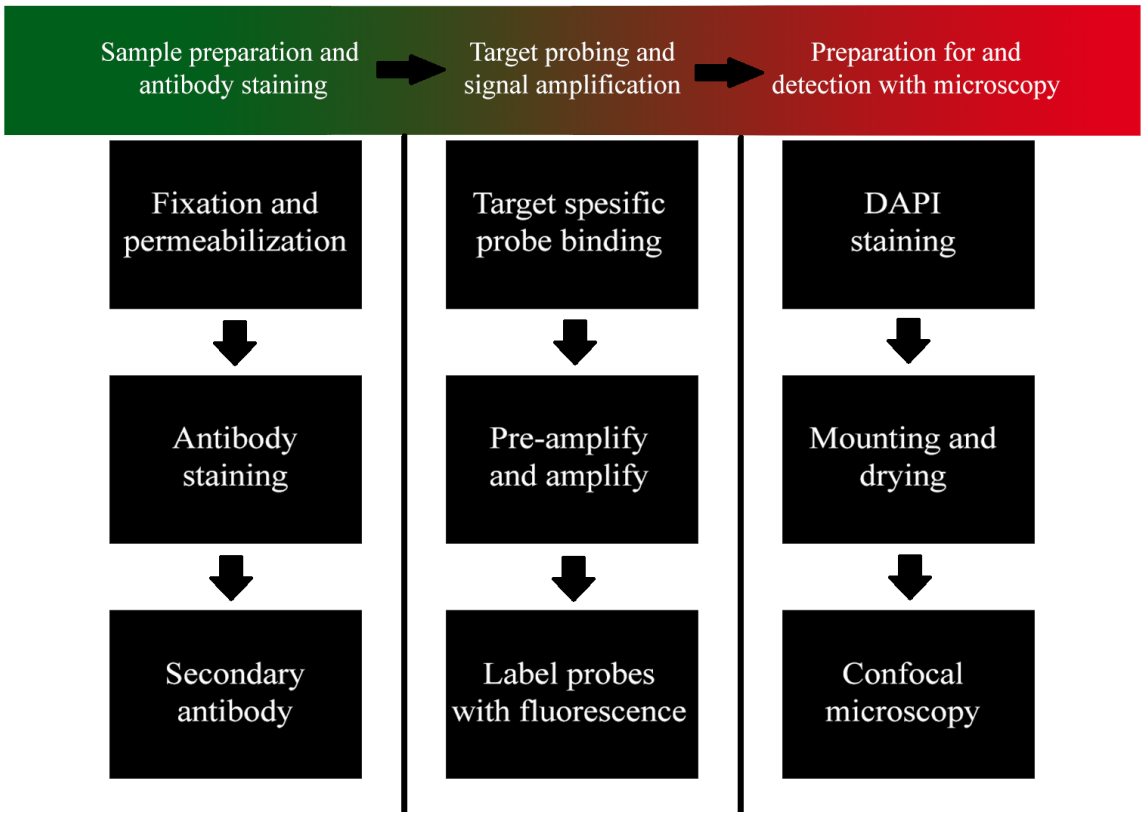

Figure 5. Workflow for the bDNA-FISH experiment. The cell samples are infected with viruses and fixed and permeabilized before staining with primary antibodies and fluorescent secondary antibodies. The viral RNA is detected with specific primary probes and amplified with the probes in the ViewRNA kit, and nuclei are stained with DAPI. The cells are then mounted on microscopy slides and visualized using a confocal fluorescence microscope.

2.5 Confocal microscopy

Before imaging the cells with the confocal microscope, the nuclei of the cells were stained with DAPI (Invitrogen/Molecular Probes, Ref. D3571) diluted 1:40 000 in 1x PBS for 5 minutes at RT, mounted on microscopy slides (Thermo Scientific) with in-house made Mowiol-Dabco (33.3% (vol/vol) glycerol containing 16.6% (wt/vol) Mowiol (Calbiochem, Ref. 475904) and 2.5% (wt/vol) 1,4-diazabicyclo[2.2.2]octane (DABCO) (Sigma Aldrich, Ref. D2, 780-2)), and stored in the dark at 4 °C overnight.

The cells were imaged using Olympus microscope IX81 with FluoView-1000 confocal setup, with the Olympus UPlanFLN 40x oil immersion objective (numerical aperture 1.30) and Olympus Immoil-F30CC immersion oil. The lasers used in the experiments were 405 nm multiline diode laser, 488 nm argon laser and 543 nm and 633 nm HeNe lasers. The following software settings were used in image acquisition: unidirectional scan mode, dwell time 4.0 µs/pixel, image size 640 x 640 pixels, aspect ratio 1:1, sequential line capture, Kalman averaging with 3 scans.

2.6 Antiviral drugs

For the RT-qPCR and bDNA FISH experiments with the antiviral drugs, the drugs were added to the 10% DMEM, which was administered to the cells right before the start of the infection. Rac1-I (Sigma Aldrich, Ref. SML0952) was used at 200 µM final concentration, Cal-I1 (Roche Diagnostics GmbH, Ref. 11086090001) was used at 200 µM final concentration and IHD (unpublished) was used at 5 µM final concentration.

2.7 RT-qPCR

The RT-qPCR experiment was started with seeding 90 000 A549 cells per well on 4-well plates. After 24 hours, the plates were infected with 1:10 000 diluted CVA9 virus as described in section 2.2 (400 µl final volume). After incubation at 37 °C for 0-5 hours, the infection was stopped by putting the plates in -80 °C.

After stopping the infection, the plates were thawed for 15 minutes at 37 °C, and frozen for 15 minutes at -80 °C. This was repeated three times to lyse the cells and release the virus without destroying the viral RNA. Cell debris (400 µl) was transferred to a 1.5 ml LoBind Eppendorf tube (Eppendorf, Ref. 0030108051) and centrifuged for 10 minutes at 16 700g with a table centrifuge (Eppendorf, Centrifuge 5415 D). 140 µl of the supernatant was used for the RNA extraction, and the rest was stored at -80 °C.

Viral RNA was extracted with QIAamp Viral RNA Mini kit (Qiagen, Ref. 52906) according to the spin protocol provided in the kit's handbook. Extracted RNA (60 µl) was stored at -80 °C.

The primers for the RT reaction and the qPCR reaction were synthesized and acquired from Thermo Scientific. The primer for the -RNA had the following sequence: 5′ -GAAACACGGACACCCAAAGTA- 3′, and the primer for the +RNA had the following sequence: 5′ -CGGCCCCTGAATGCGGCTAA- 3′. The sequences for the primers were originally received from Matti Waris (University of Turku) and the sequences have been successfully used before to detect enterovirus RNAs.

The RT reaction was performed by making a master mix (Table 2) without the RNA template for all samples, aliquoting 30 µl of the master mix to 1.5 ml tubes and adding 10 µl of the extracted RNA template to the tubes. Template and the master mix were thoroughly mixed in the tube and incubated for 1 hour at 42 °C, following a heat-inactivation of the RT enzyme for 10 minutes at 70 °C. The acquired cDNA was diluted 1:100 in nuclease-free water and stored at -20 °C.

Control reactions for the RT-qPCR experiment included negative controls for RNA extraction, negative controls for the RT reaction and negative controls for the qPCR reaction. In negative controls, we used nuclease free water (Alfa Aesar, Ref. J71786) instead of the template RNA/cDNA.

Table 2. Components of the RT reaction.

Reagent	Amount (µl) per sample	Final concentration	Origin
Nuclease free water	9.0	-	Alfa Aesar (Ref. J71786)
5x RT-buffer	8.0	1x	Promega (Ref. M5301)
2.5 mM dNTP mix with dATP, dTTP, dCTP and dGTP	8.0	0.5 mM each	Promega (Ref. U1330)
10 µM ENRI (3+ or 4-) primer	4.8	1.2 µM	Thermo Scientific Custom Standard DNA Oligos
RNase inhibitor	0.1	4 units	Promega (Ref. N2518)
RT-enzyme (M-MLV RT [H–])	0.1	20 units	Promega (Ref. M530A)
RNA template	10.0	-	Viral RNA extraction
Total	**40.0**	**-**	**-**

The qPCR was performed by making a master mix (Table 3) without the cDNA template for all samples, aliquoting 20 µl the master mix to wells on PCR-plates (Bio-Rad, Ref. HSL9601) and adding 5 µl of the cDNA template to the wells. Triplicate wells were made for all samples. Template and the master mix were thoroughly mixed in the wells, and the plate was carefully sealed with a PCR plate tape (Bio-Rad, Ref. MSB1001). The qPCR was performed with a Bio-Rad CFX96 Touch Real-Time PCR Detection System with the following protocol:

1. Initial denaturation: 95 °C, 10 minutes
2. Denaturation: 95 °C, 15 seconds
3. Annealing, extension, plate read: 60 °C, 1 minute
4. Repeat steps 2-3 for 39 more times
5. End of the run and hold: 12 °C, 10 minutes

Table 3. Components of the qPCR reaction.

Reagent	Amount (µl) per sample	Final concentration	Origin
Nuclease free water	4.5	-	Alfa Aesar (Ref. J71786)
iQ SYBR Green Supermix	12.5	1x	Bio-Rad (Ref. 1708886)
10 µM ENRI 4- primer	1.5	0.6 µM	Thermo Scientific Custom Standard DNA Oligos
10 µM ENRI 3+ primer	1.5	0.6 µM	Thermo Scientific Custom Standard DNA Oligos
cDNA template	5.0	1:500	RT-reaction
Total	**25.0**	**-**	**-**

2.8 Image and data processing

The images acquired from the confocal microscope were refined and analysed with Fiji v. 1.52s, a distribution of the ImageJ image processing software (Schindelin et al., 2012). First, all images were converted to 8-bit images to have comparable intensity values between 1 and 256. The minimum intensity value of uninfected negative control cell images was manually set so high that the image was completely blank, using a Hi-Lo lookup table. This minimum intensity threshold was then applied to all the sample images, effectively removing background fluorescence. In addition, a 1.0-pixel radius mean filter was applied to the images to remove unwanted background noise. Equal amounts of brightness was also applied to all images to make the signals clearer while keeping the amounts of signal comparable between images.

Intensity calculations from bDNA FISH images were acquired by using the "Measure" tool with "Limit to threshold" in Fiji after thresholding the background as explained above. One field view image per sample with ~100 cells per image was

used for the calculations. The measurement calculates the area of all pixels that have intensity values above the set threshold, which is a quantitation of the amount of intensity in the sample image, assuming that all pixels with intensity values above the threshold value are positive signals from the bDNA FISH.

For the RT-qPCR data, average Cq values were calculated from the triplicate measurements for each sample and plotted as a bar chart with standard deviation error bars representing the amount of variance in the Cq values in the triplicates.

3 RESULTS

Initially we did bDNA FISH experiments with the viruses CVA9, CVB3 and EV1 to see which virus would be the most suitable model for the study. The results (not shown here) indicated that CVA9 had the most +RNA and -RNA visible under a confocal microscope out of the three enteroviruses, making it our choice of virus for the study. The rest of the experiments were carried out with the CVA9 virus only.

During the optimization of the bDNA FISH method we discovered that the -RNA was barely visible under the confocal microscope, possibly due to the +RNA and -RNA strands making double stranded RNA intermediates, effectively inhibiting the binding of our RNA probes to the strands. To overcome this problem, we tested 100% methanol, up to 8 molar urea and 95% formamide in 0.1x SSC buffer to separate the strands from each other. The results (not shown here) indicated that 100% methanol and urea at 1-8 molar concentrations did not affect the visibility of either RNA strand, but 95% formamide in 0.1x SSC buffer improved the visibility of the -RNA significantly. Using high temperature combined with 95% formamide to separate the RNA strands from each other has been shown to improve the visibility of poliovirus -RNA in FISH based methods (Bolten et al., 1998), and the use of this method was critical for the success of our bDNA FISH experiments.

None of the negative controls used for RT-qPCR crossed the Cq value threshold, proving that the samples were not contaminated by other RNA- or DNA molecules.

3.1 Distribution of enterovirus +RNA and -RNA in relation to the capsid during an infection

In our first experiments we used bDNA FISH and standard antibody-based immunofluorescence to label the CVA9 capsid protein VP1, double stranded RNA (dsRNA) and either +RNA or -RNA, at timepoints of 1, 2, 3, 4 and 5 hours post infection (p.i.). The results indicate that the amount of viral capsid protein is negligible before 4 h p.i., and most of the capsid protein is located peripherally in the cell (Figures 6 and 7). The +RNA is visible even at 1h p.i., but the amount of

visible +RNA surges at 3h p.i. and gradually rises at 4h and 5h p.i (Figure 6). These results suggest that the visible +RNA at 1-2h p.i. originates from the input virus, which means that the virus does not start replicating +RNA until after 2-3h p.i. The +RNA in the cell is located even more peripherally than the capsid protein, and there is very little colocalization with the +RNA and the capsid protein. The dsRNA visible in figures 6 and 7 is not reliable, as the fluorescent secondary antibody (GAM633, Table 1) used to detect the primary dsRNA antibody produced visible spots even in uninfected control cells. Better, more reliable images of the dsRNA with a different secondary antibody (GAM488, Table 1) can be found in figure 8.

In the samples where we labelled -RNA instead of +RNA, the amount of -RNA is negligible at timepoints 1h - 3h p.i., but some -RNA can be seen after 4h p.i. (Figure 7). As with the +RNA samples, the capsid becomes visible at 3-4h p.i., and is located peripherally in the cell. The -RNA is located more closely to the nucleus than the capsid protein, and the -RNA does not colocalize with the capsid protein at all.

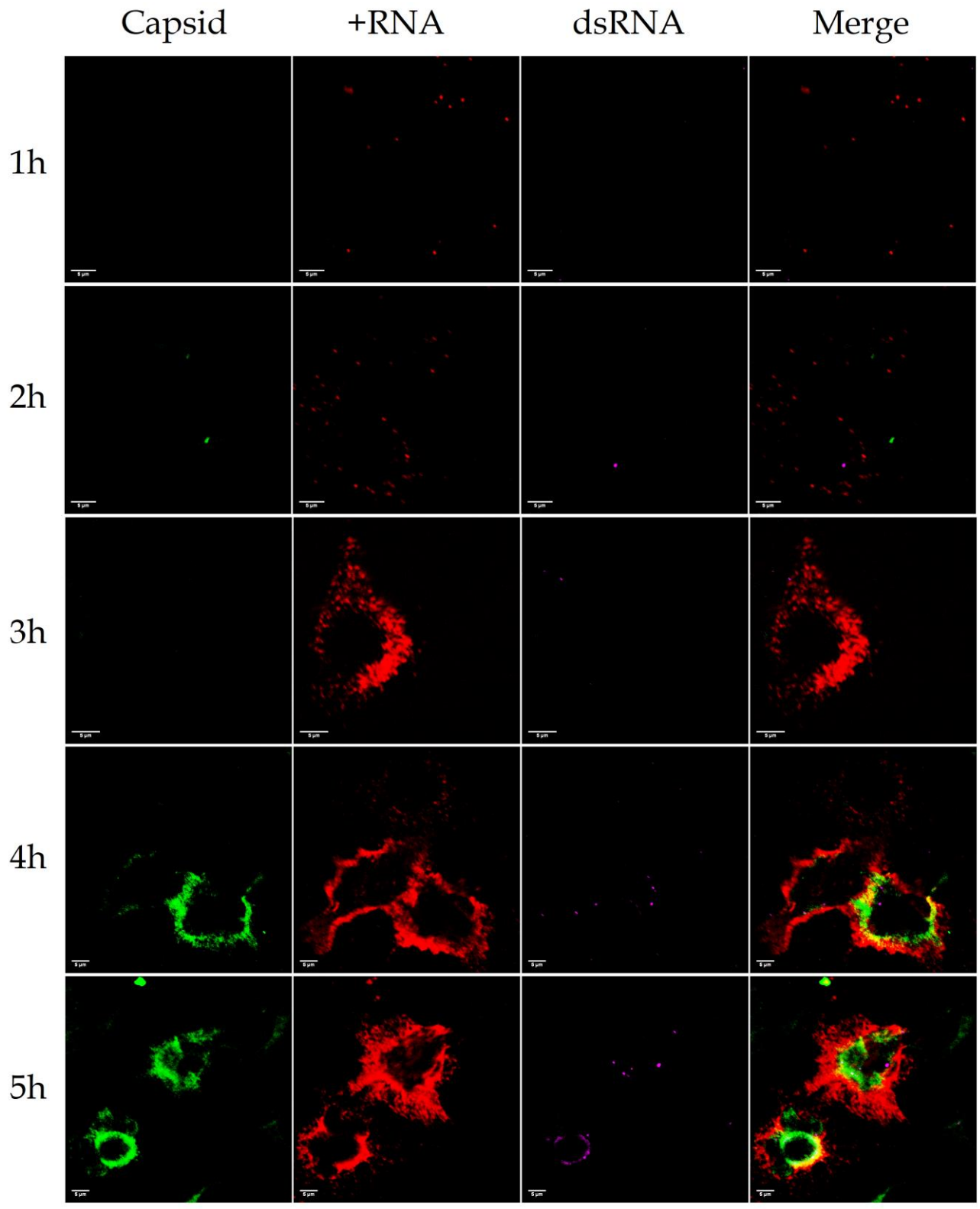

Figure 6. Distribution of viral +RNA, dsRNA and capsid protein in CVA9 infected cells 1-5h p.i. The capsid protein is shown in green, +RNA is shown in red and dsRNA is shown in magenta. The rows from top to bottom are 1h, 2h, 3h, 4h and 5h p.i. Capsid protein becomes visible after 4h p.i. and +RNA is visible at all timepoints, but surges in visibility at 3h p.i. The capsid and the +RNA mostly reside in separate locations. The dsRNA shown here is not reliable as there were visible dsRNA spots in uninfected control cells. Scale bar in every image is 5 µm.

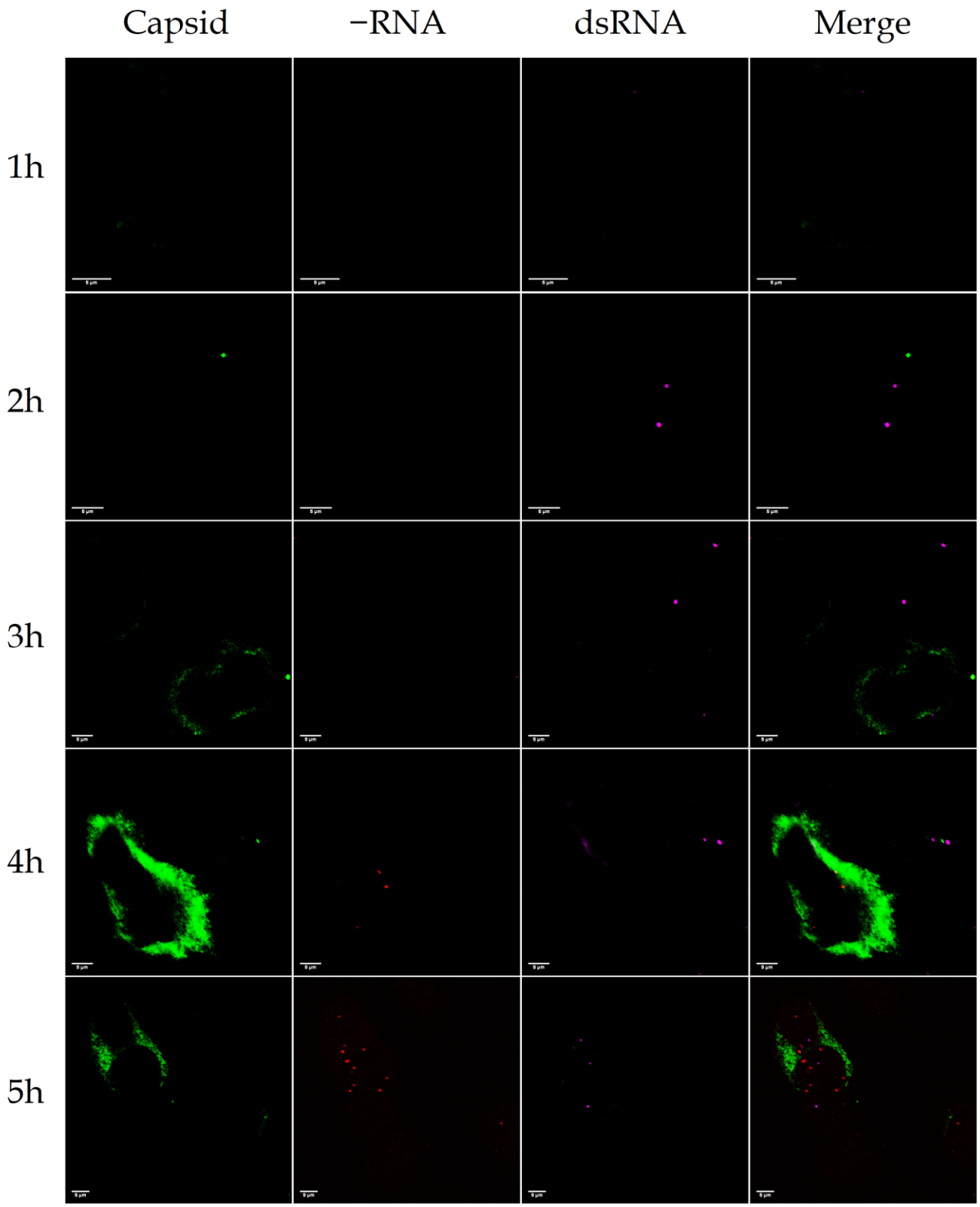

Figure 7. Distribution of viral -RNA, dsRNA and capsid protein in CVA9 infected cells 1-5h p.i. The capsid protein is shown in green, -RNA is shown in red and dsRNA is shown in magenta. The rows from top to bottom are 1h, 2h, 3h, 4h and 5h p.i. Capsid protein becomes visible after 3-4h p.i. and -RNA becomes visible at 4h p.i. There is no colocalization between the capsid and the -RNA. The dsRNA shown here is not reliable as there were visible dsRNA spots in uninfected control cells. Scale bar in every image is 5 µm.

3.2 Distribution of enterovirus +RNA, -RNA and dsRNA during an infection

In the second experiment, we simultaneously labelled viral dsRNA, -RNA and +RNA from cells infected with CVA9 at timepoints 0.5, 1, 2, 3, 4 and 5h p.i. (Figure 8). The results are similar to the first experiments, with -RNA becoming visible at 3 - 4h p.i., input +RNA being visible at 0.5 - 2h p.i. and the amount of +RNA surging at 3h p.i. The amount of visible dsRNA is negligible at timepoints 0.5 - 2h p.i., but surges in visibility at 3h p.i.

According to our results, the dsRNA resides in the same location as +RNA and mostly in the same location as the -RNA. The -RNA also resides in the same location with the +RNA, but since the +RNA signal is quite ubiquitous in the cell, the colocalization of +RNA with -RNA and dsRNA is debatable. The dsRNA and -RNA are more centrally located in the cell around the nucleus than the peripherally located +RNA. None of the RNA signals localize in the nuclei of the cells.

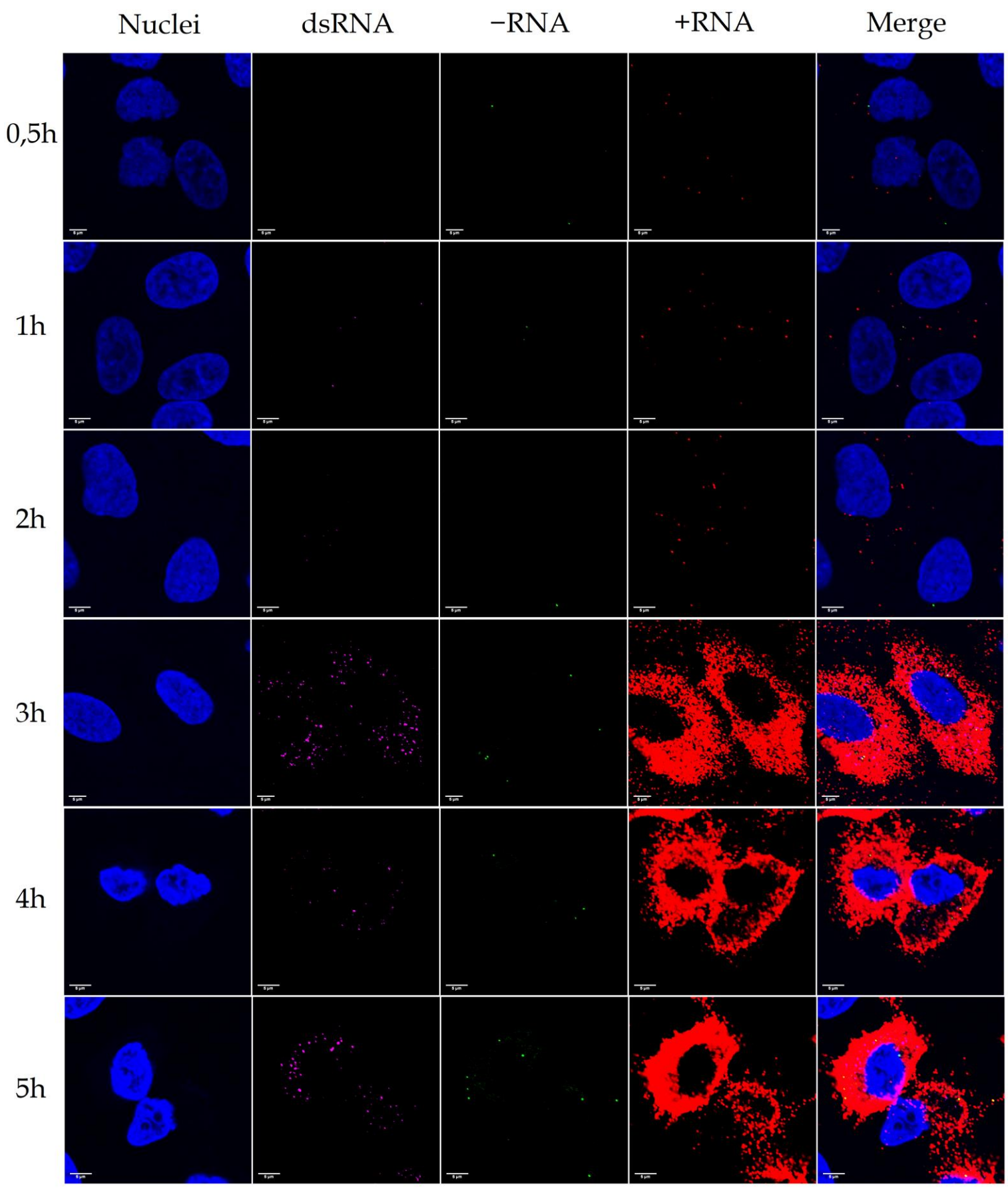

Figure 8. Distribution of viral -RNA, +RNA and dsRNA in CVA9 infected cells 0.5 - 5h p.i. Nuclei are shown in blue, dsRNA is shown in magenta, -RNA is shown in green and

+RNA is shown in red. The rows from top to bottom are 0.5, 1, 2, 3, 4 and 5h p.i. Some dsRNA can be seen at 0.5 - 2h p.i., but the amount of dsRNA surges at 3h p.i. The amount of -RNA at timepoints 0.5h - 2h p.i is negligible, but some -RNA can be seen at timepoints 3h - 5h p.i. The +RNA from the input virus can be seen at timepoints 0.5h - 2h p.i., and the amount of +RNA surges at 3h p.i. and gradually increases at timepoints 4h and 5h p.i. The -RNA seems to mostly colocalize with the dsRNA and +RNA, and dsRNA colocalizes with +RNA. Scale bar in every image is 5 µm.

3.3 The amounts of enterovirus +RNA and -RNA during an infection

We used RT-qPCR to detect the amounts of enterovirus RNA molecules in CVA9 infected cells at timepoints 0, 1, 2, 3, 4 and 5h p.i. (Figure 9). The results are presented in Cq values, which means the amount of PCR cycles it takes for the RNA to cross a detectable threshold, meaning that the lower the value is, the more RNA there is in the sample. The results are in line with the bDNA FISH experiments, with the amount of -RNA being considerably lower than the amount of +RNA, and the amounts of both +RNA and -RNA increasing dramatically at 3-4h p.i.

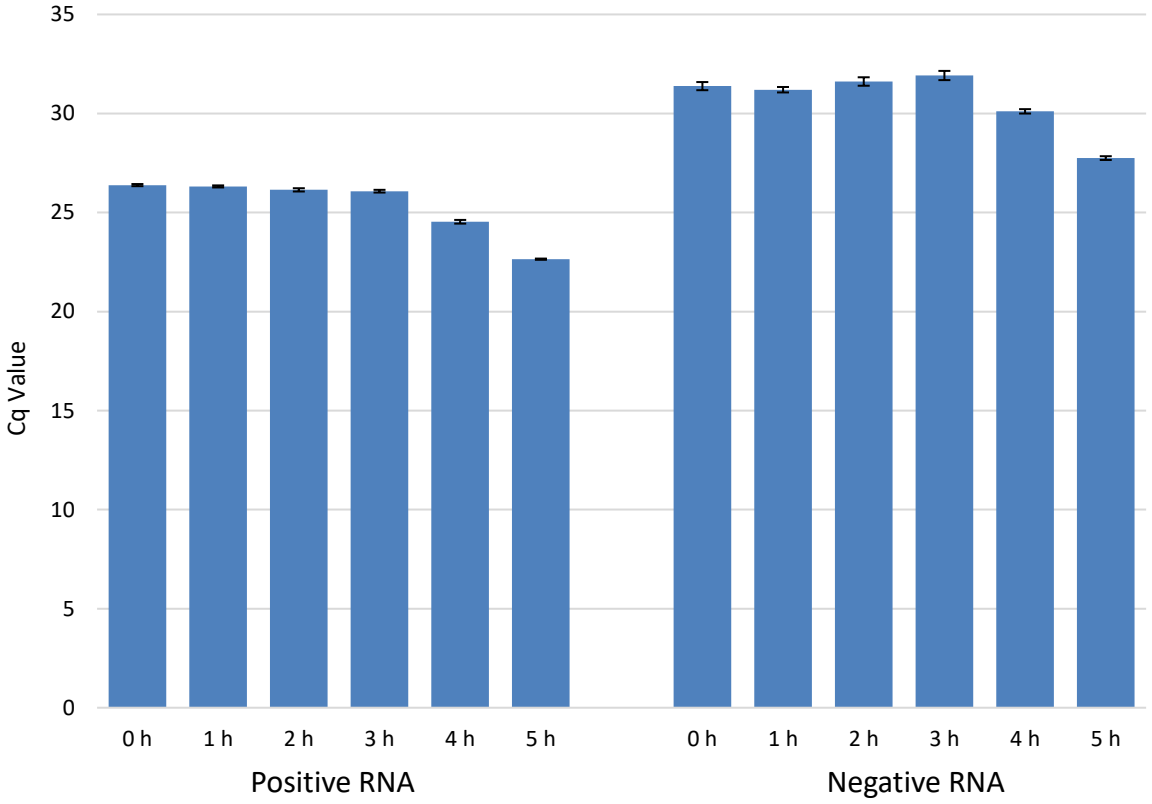

Figure 9. The amount of viral +RNA and -RNA in CVA9 infected cells at timepoints 0-5h p.i. The amount of +RNA at timepoints 0-5h p.i. is shown on the left, and the amount of -RNA at timepoints 0-5h p.i. is shown on the right. The bars are averages calculated from triplicate samples, and the error bars are standard deviations from the average values.

The amounts of enterovirus RNAs were also calculated from intensity values of the bDNA FISH sample pictures using Fiji. The results are presented in pixels that have intensity values above the set threshold plotted against time (Figures 10 and 11). The results are quite similar to the results from our qPCR experiments, showing exponential growth in the amounts of both RNAs. It is noteworthy to mention that the results are calculated from only ~100 cells per sample. These results confirm that there is approximately a 100-fold difference in the amounts of enterovirus -RNA and +RNA consistently throughout the infection.

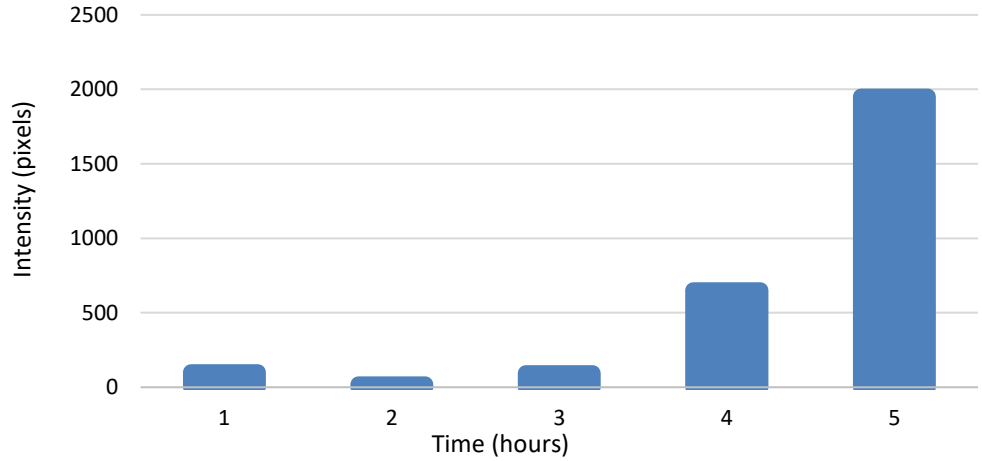

Figure 10. The amount of viral +RNA in CVA9 infected cells at timepoints 0-5h p.i. as calculated from bDNA FISH image intensity values. The bars represent pixels that have intensity values above the background threshold, calculated from one field view picture with ~100 cells in it.

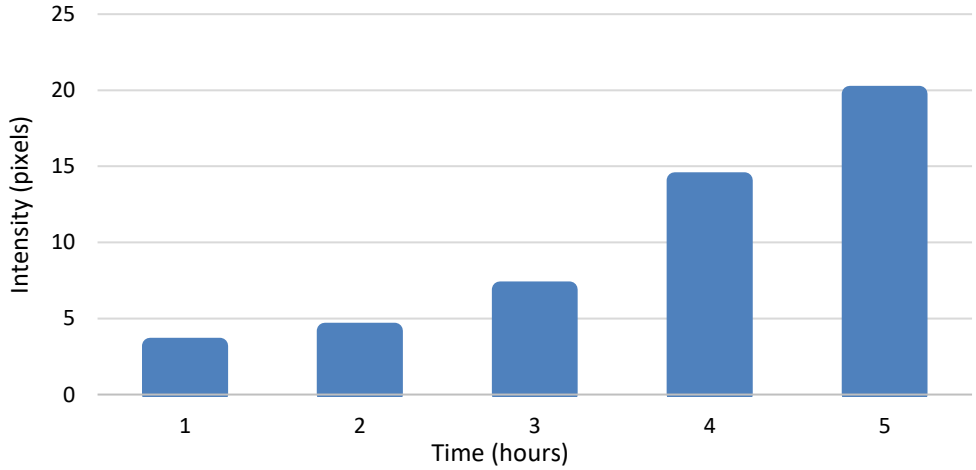

Figure 11. The amount of viral -RNA in CVA9 infected cells at timepoints 0-5h p.i. as calculated from bDNA FISH image intensity values. The bars represent pixels that have intensity values above the background threshold, calculated from a field view picture with ~100 cells in it.

3.4 Effect of antiviral drugs on the amounts of viral +RNA and -RNA

We tested the effect of the antiviral drugs Rac1-I, Cal-I1 and IHD on the amount of enterovirus +RNA and -RNA molecules being produced in CVA9 infected cells at 5h p.i. (Figure 12). The results show that all of the drugs lowered the amount of viral +RNA and -RNA molecules to the levels of 0h infected cells (only input virus, no incubation period) and there was very little variation in the efficiency of the drugs.

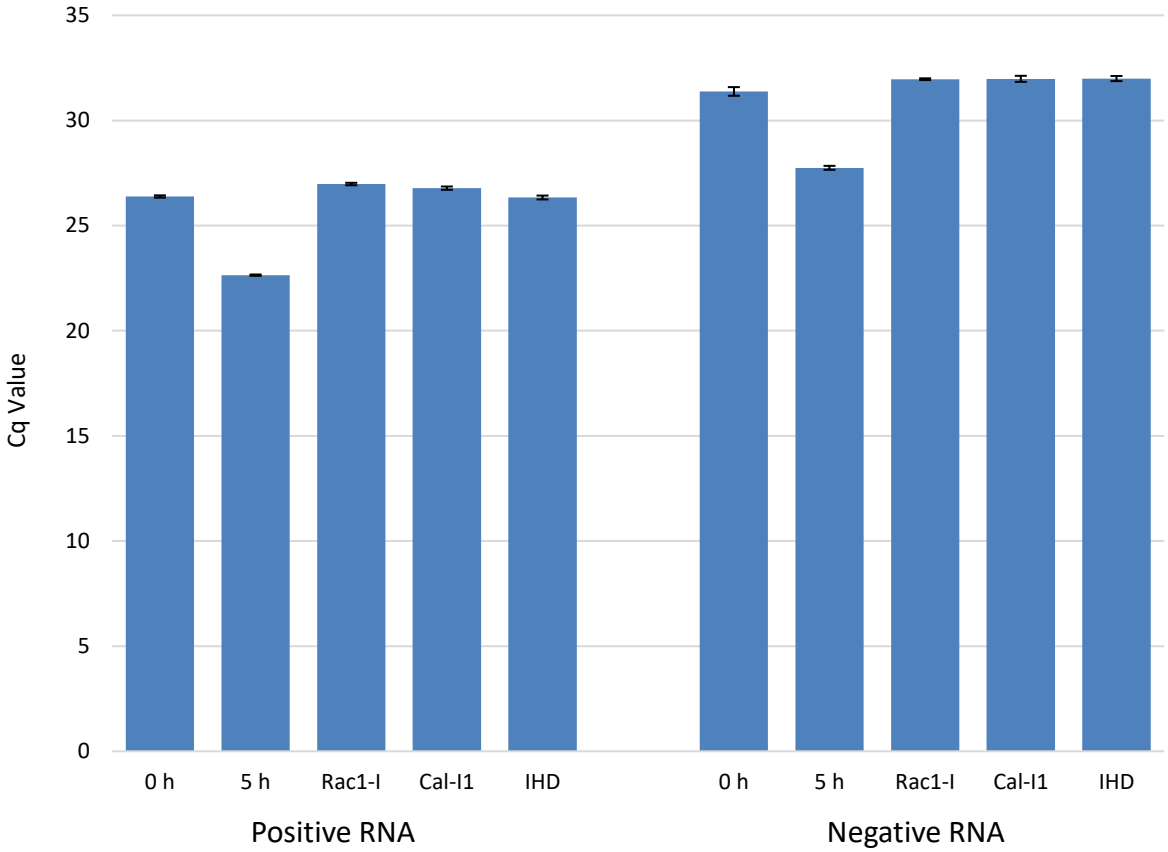

Figure 12. The effect of antiviral drugs Rac1-I, Cal-I1 and IHD on the amounts of enterovirus +RNA and -RNA in CVA9 infected cells at 5h p.i. The amount of +RNA is shown on the left (samples from left to right: 0h p.i. with no drugs, 5h p.i. with no drugs, 5h p.i with Rac1-I, 5h p.i. with Cal-I1, 5h p.i. with IHD), and the amount of -RNA is shown on the right with the samples in the same order. The bars are averages calculated from triplicate samples, and the error bars are standard deviations from the average values.

3.5 Effect of antiviral drugs on the distribution of viral +RNA and -RNA

We infected cells with CVA9 while the cells were under the effects of either Rac1-I, Cal-I1 or IHD, and then simultaneously labelled the viral dsRNA, +RNA and -RNA at timepoints 0.5h p.i. and 5h p.i. (Figure 13).

The results indicate that Rac1-I completely blocks the virus infection in most cells, but some cells do still get infected (Figure 13, panel A). In the infected cells, the levels of all RNA molecules have dropped considerably, but the localization and colocalization of the RNA molecules seem to stay the same.

Cal-I1 seems to be the most effective drug of the three tested, blocking the virus infection completely in almost all cells (Figure 13, panel B). Some cells show input virus - levels of +RNA, and no dsRNA or -RNA at all.

The IHD completely blocks the infection in most cells, but some cells exhibit input-virus levels of +RNA. (Figure 13, panel C). Some cells also exhibit high levels of all viral RNA molecules, but this is most probably due to leaking of the drug molecule.

In all three drug-treated samples, the amount of viral RNA molecules has dropped significantly (Figure 12). Even though the RT-qPCR data suggests that the amounts of viral RNA in drug-treated samples are on the level of just input virus (0h p.i.), the bDNA FISH shows some degrees of infection in both Rac1 and IHD treated cells (Figure 13, panels A and C). The percentage of infected cells in all drug-treated bDNA FISH samples is very low, explaining the contradiction between the RT-qPCR data and the bDNA FISH data.

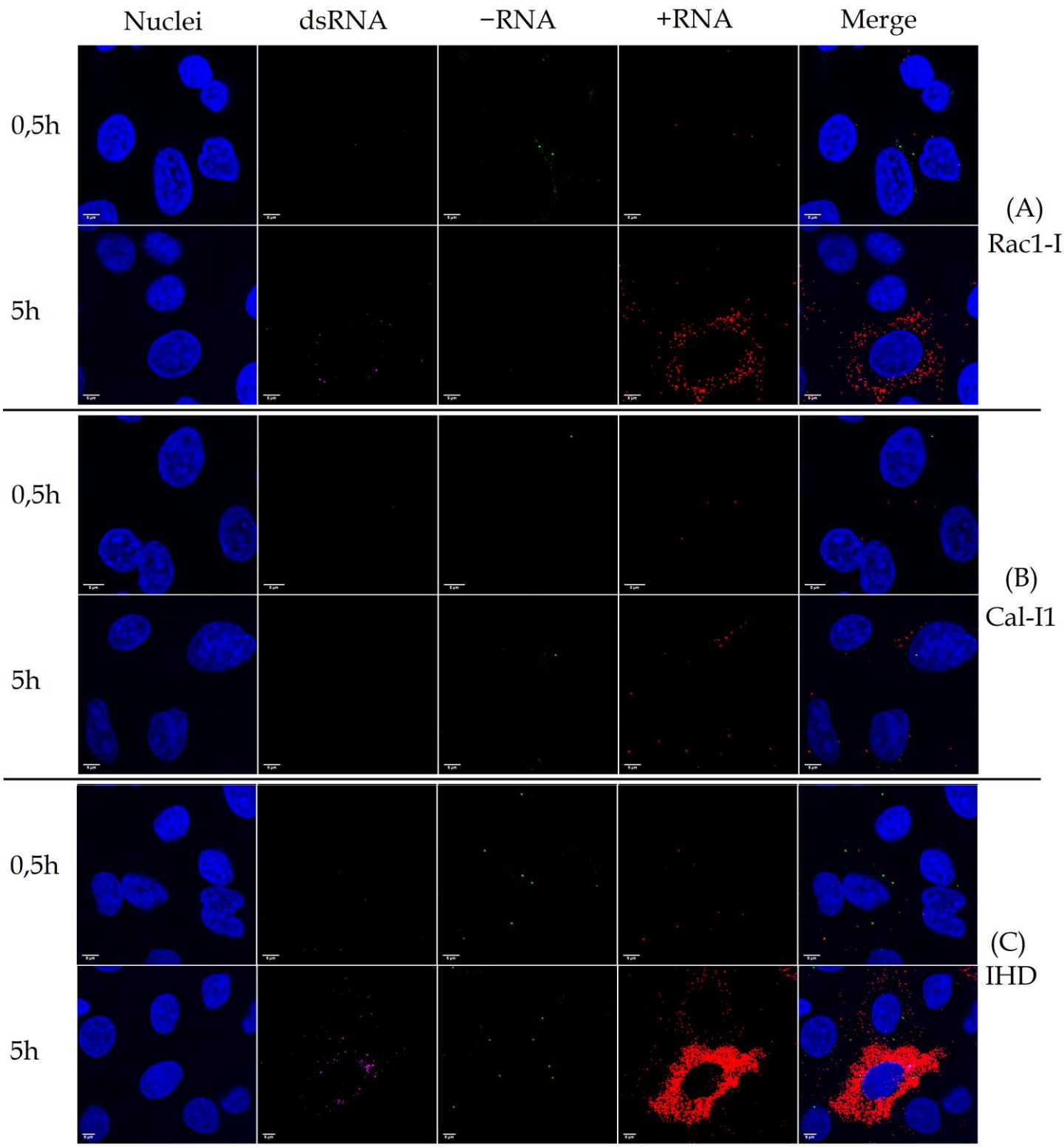

Figure 13. Effect of antiviral drugs Rac1-I, Cal-I1 and IHD on the distribution on viral dsRNA, -RNA and +RNA in CVA9 infected cells at timepoints of 0.5h and 5h p.i. Nuclei are shown in blue, dsRNA in magenta, -RNA in green and +RNA in red. **(A)** Rac1-I inhibits the virus infection completely in most cells, but some cells exhibit input-virus levels of +RNA. **(B)** Cal-I1 inhibits the virus infection completely in almost all cells. **(C)** IHD inhibits the virus infection completely in most cells, but some cells exhibit input-virus levels of +RNA. A few cells also exhibit levels of RNAs comparable to non-drugged infected cells, probably due to leaking of the drug molecule.

4 DISCUSSION

Enteroviruses, a genus of the *Picornaviridae* family, are small, non-enveloped viruses with a single-stranded positive-sense RNA genome. While their life cycle is relatively well-known, the distribution and the amounts of the viral +RNA and -RNA strands during an infection was clouded due to insufficient methods to study them. Here we have shown that the amounts of both +RNA and -RNA are negligible before 3-4 hours p.i. (Figure 9), meaning that the entry and uncoating of the virus particle and the initial translation of the input +RNA strand takes around 3-4 hours. After this, the replication process starts and the amounts of both +RNA and -RNA surge dramatically at 4 hours p.i. and 5 hours p.i. These results are in line with previous studies stating that the majority of uncoating of CVA9 happens around 2 hours p.i., while the replication cycle starts around 3 hours p.i. (Huttunen et al., 2014).

Assuming that the efficiency of our qPCR is close to 100%, the amount of cDNA (from the viral RNA) is doubled every PCR cycle. This can be presented with the equation $2^x = y$, where X is the number of PCR cycles and Y is fold change. This can be further solved to $x = log_2 y$, which solves further in to $x = \frac{\log y}{\log 2}$. Now if we want to solve how much is 3 cycles of PCR in fold change, we substitute X with the number 3, giving us the answer 8. This means that 3 cycles of PCR is roughly equivalent to an 8-fold amplification of cDNA.

We measured a 5-6 cycle difference in -RNA and +RNA amounts at all timepoints (Figure 9), translating to around 32-fold to 64-fold difference between the amounts of -RNA and +RNA. However, since RT-qPCR does not give absolute amounts of measured RNAs, these results are only rough estimations. To better estimate the difference in the amounts of enterovirus -RNA and +RNA throughout the infection, we calculated the intensity values of the RNAs from the bDNA FISH images (Figures 10 and 11). The results showed that there is a 100-fold difference in the amounts of enterovirus -RNA and +RNA consistently throughout the infection,

confirming previous estimations of a 40- to a 100-fold difference (Novak and Kirkegaard, 1991).

The amounts of -RNA and +RNA compared to the timepoint 0h p.i. (background level) were calculated with the aforementioned equation and plotted against time 0h - 5h p.i. (Figure 14). The fold changes of both RNAs during early infection (1h - 3h p.i.) are negligible. At 4h p.i., the amount of +RNA is 3.6 times higher (compared to 0h p.i.) and the amount of -RNA is 2.4 times higher, and at 5h p.i. the amount of +RNA is 13.4 times higher and the amount of -RNA is 12.4 times higher. We expected to see an increase in the amount of -RNA before the increase of +RNA, and that the pace at which the -RNA is replicated would drop off once the replication of +RNA starts, but that seems to not be the case. Interestingly, our results show that the amounts of +RNA and -RNA increase at roughly the same pace, and that the replication of both RNAs starts at around 3-4 hours. Moreover, the replication pace of either of the RNAs does not slow down at any point during the infection, even though the -RNA is not used for anything after the replication process is complete.

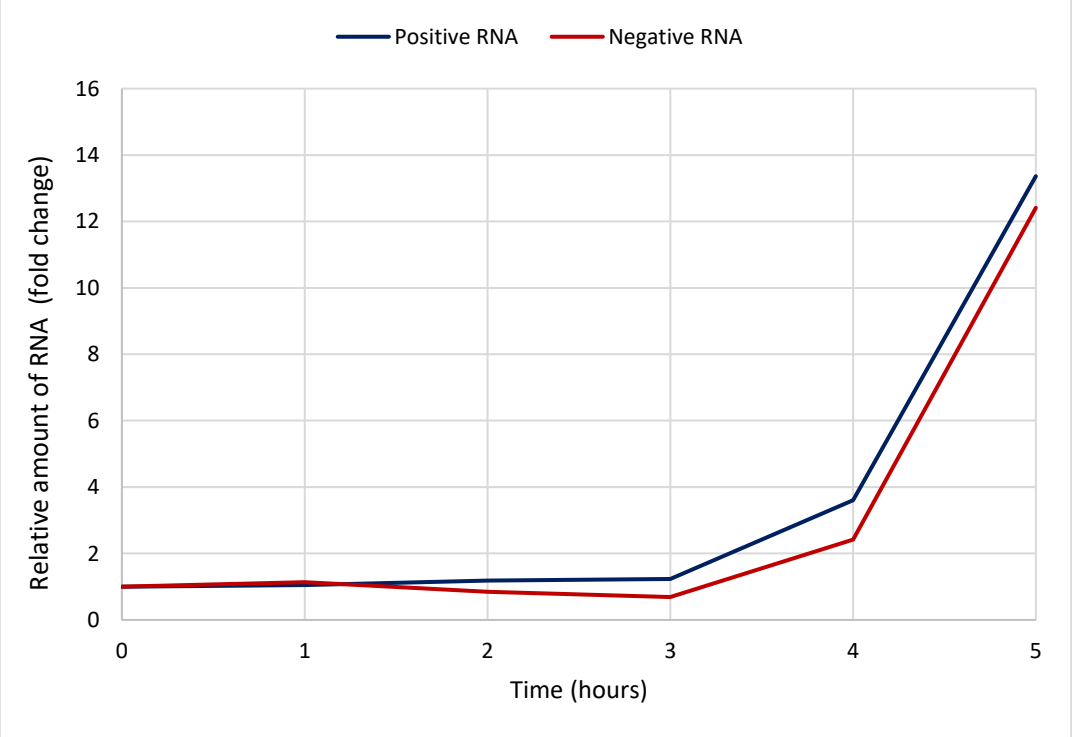

Figure 14. The change in the relative amounts of viral +RNA and -RNA during a CVA9 infection compared to timepoint 0h p.i. The X-axis shows the time post-infection, and Y-axis shows fold change (how many times higher the amount of RNA is compared to 0h p.i.). The +RNA is shown in blue, and -RNA is shown in red. The pace at which the amounts of RNAs increase is almost identical.

Since enterovirus virions have no inherent -RNA strands, the RT-qPCR studies should give no Cq value at all for the -RNA at 0h p.i. However, we did get values for the -RNA at 0h p.i. in our study (Figures 9 and 12), even though we did not get values for any negative control reactions, indicating that false-priming is responsible for the values we see. It has been shown for enteroviruses that false-priming, an event in which the viral RNA uses other RNA molecules as primers to synthesize cDNA during the reverse transcription step of RT-qPCR, can lead to false positive results and/or overestimation of the actual quantity of RNA molecules present in the sample (Bessaud et al., 2008). False-priming is most probably the reason we see the low amounts of -RNA at 0h p.i. in our results, but since false-priming happens in all of the samples, the results are still comparable with each other. In future studies, it is recommended to take measures (such as tagged RT-qPCR suggested by Bessaud et al.) to avoid false-priming in RT-qPCR.

We demonstrated the use of bDNA FISH in the study of enterovirus RNA strands during an infection and established a working protocol for the method. Even though we had some problems with the visibility of the -RNA, the use of 95% formamide in 0.1x SSC-buffer improved the visibility enough that we were able to study the -RNA effectively. As mentioned, we also tested 100% ice-cold methanol and up to 8M urea, but these chemicals had no effect on the visibility of the -RNA. It has been reported that dimethyl sulfoxide (DMSO) is more effective than formamide in the separation of DNA strands (Wang et al., 2014), but unfortunately, we did not have time to test DMSO in our study. Due to the fragility of RNA, physical separation methods such as beads mill or sonication will probably not work with this protocol, but DMSO could provide a safer and more effective visibility improving agent for bDNA FISH than formamide does. More studies are needed to properly characterize the effects of DMSO on the visibility of enterovirus -RNA strands while using bDNA FISH.

Since the ViewRNA Assay Kit allows the labelling of only three different molecules, we unfortunately could not label the capsid, +RNA, -RNA and dsRNA all at once. However, our results suggest that the -RNA and dsRNA, which take part only in replication, are located quite centrally in the cell, indicating that the virus'

replication organelles are located centrally in the cell as well. Along with capsid proteins, the +RNA is located peripherally (but also quite ubiquitously later in the infection) in the cell, indicating that the assembly of new virus particles takes place in the cell periphery. Since the dsRNA colocalizes fully with +RNA and mostly with -RNA, we suspect that most of the dsRNA strands we see are replication intermediates. Enteroviruses do also produce stable replicative form dsRNA structures, whose function is yet to be discovered (Paul, 2002).

We demonstrated that the antivirals Rac1-I, Cal-I1 and IHD effectively block the CVA9 infection in cells *in vitro* at concentrations 200 µM, 200 µM and 5 µM, respectively. It is noteworthy to mention that the pictures taken from the bDNA FISH experiment with the antivirals give only a glimpse of the reality; even though the amount of RNAs in Figure 13 might seem high, only a small percentage of cells exhibit viral RNAs. The RT-qPCR experiment (Figure 12) gives a better idea of the effectiveness of the antivirals tested. In the cells that were infected, the antivirals did not seem to change the distribution or localization of the RNA molecules at all. Nevertheless, we have shown here that bDNA FISH and RT-qPCR are both suitable methods for studying the effects of antiviral drugs on cells infected with enteroviruses. The three drugs we tested are promising *in vitro*, but require more studies to study their toxicity, their effectiveness at lower concentrations, and possible delivery methods *in vivo*.

The lifecycle of enteroviruses is a bit clearer now as a result of this study, telling us that the replication of the viral RNA starts 2-3 hours after infection and the translation of RNA to capsid proteins starts shortly after at 3-4 hours post-infection. The results also indicate that the virus' replication organelles (ROs) are located quite centrally in the cell, while the virion assembly most likely takes place in the periphery of the cell. These findings are consistent with earlier literature describing ROs being usually located in the inner endoplasmic reticulum (Melia et al., 2019; Romero-Brey and Bartenschlager, 2016) and virion assembly taking place at the peripheral endoplasmic reticulum (Romero-Brey and Bartenschlager, 2016). We also discovered that the pace of replication of -RNA and +RNA strands is almost identical, contradictory to earlier beliefs of +RNA synthesis being faster paced than

-RNA synthesis (Paul, 2002). Considering these results, new antiviral drugs can be designed more efficiently to target the various steps of the enterovirus life cycle. Moreover, the bDNA FISH protocol we established can be easily and readily applied to study enterovirus RNAs more efficiently.

REFERENCES

Baggen J., Thibaut H.J., Starting J.R.P.M & van Kuppeveld F.J.M. 2018. The life cycle of non-polio enteroviruses and how to target it. *Nature Reviews Microbiology* 16: 368-1526.

Basavappa R., Syed R., Flore O., Icenogle J.P., Filman D.J. & Hogle J.M. 1994. Role and mechanism of the maturation cleavage of VP0 in poliovirus assembly: structure of the empty capsid assembly intermediate at 2.9 A resolution. *Protein science: a publication of the Protein Society* 3: 1651-1669.

Battich N., Stoeger T. & Pelkmans L. 2013. Image-based transcriptomics in thousands of single human cells at single-molecule resolution. *Nat Methods* 10: 1127-1133.

Bessaud M., Autret A., Jegouic S., Balanant J., Joffret M. & Delpeyroux F. 2008. Development of a Taqman RT-PCR assay for the detection and quantification of negatively stranded RNA of human enteroviruses: Evidence for false-priming and improvement by tagged RT-PCR. *J Virol Methods* 153: 182-189.

Bolten R., Egger D., Gosert R., Schaub G., Landmann L. & Bienz K. 1998. Intracellular localization of poliovirus plus- and minus-strand RNA visualized by strand-specific fluorescent In situ hybridization. *J Virol* 72: 8578-8585.

Bozym R.A., Morosky S.A., Kim K.S., Cherry S. & Coyne C.B. 2010. Release of intracellular calcium stores facilitates coxsackievirus entry into polarized endothelial cells. *PLoS pathogens* 6: e1001135

Dierkes R., Warnking K., Liedmann S., Seyer R., Ludwig S. & Ehrhardt C. 2014. The Rac1 Inhibitor NSC23766 Exerts Anti-Influenza Virus Properties by Affecting the Viral Polymerase Complex Activity. *PLOS ONE* 9: e88520.

Etienne-Manneville S. & Hall A. 2002. Rho GTPases in cell biology. *Nature* 420: 629-635.

Gao Y., Dickerson J.B., Guo F., Zheng J. & Zheng Y. 2004. Rational design and characterization of a Rac GTPase-specific small molecule inhibitor. *Proc Natl Acad Sci U S A* 101: 7618.

Harris K.G. & Coyne C.B. 2014. Death waits for no man – Does it wait for a virus? How enteroviruses induce and control cell death. *Cytokine Growth Factor Rev* 25: 587-596.

Head J.R., Collender P.A., Lewnard J.A., Skaff N.K., Li L., Cheng Q., Baker J.M., Li C., Chen D., Ohringer A., Liang S., Yang C., Hubbard A., Lopman B. & Remais J.V. 2019. Early Evidence of Inactivated Enterovirus 71 Vaccine Impact Against Hand, Foot, and Mouth Disease in a Major Center of Ongoing Transmission in China, 2011–2018: A Longitudinal Surveillance Study. *Clin Infect Dis*: ciz1188.

Hober D. & Sauter P. 2010. Pathogenesis of type 1 diabetes mellitus: interplay between enterovirus and host. *Nature Reviews Endocrinology* 6: 279.

Huttunen M., Waris M., Kajander R., Hyypiä T. & Marjomäki V. 2014. Coxsackievirus A9 infects cells via nonacidic multivesicular bodies. *J Virol* 88: 5138-5151.

Karjalainen M., Kakkonen E., Upla P., Paloranta H., Kankaanpää P., Liberali P., Renkema G.H., Hyypiä T., Heino J. & Marjomäki V. 2008. A Raft-derived, Pak1-regulated Entry Participates in α2β1 Integrin-dependent Sorting to Caveosomes. *Mol Biol Cell* 19: 2857-2869.

Kralik P. & Ricchi M. 2017. A Basic Guide to Real Time PCR in Microbial Diagnostics: Definitions, Parameters, and Everything. (Report). *Frontiers in Microbiology* 8.

Laajala M., Hankaniemi M.M., Määttä J.,A.E., Hytönen V.,P., Laitinen O.H. & Marjomäki V. 2019. Host Cell Calpains Can Cleave Structural Proteins from the Enterovirus Polyprotein. *Viruses* 11: 1106.

Lai J.K.F., Sam I. & Chan Y.F. 2016. The Autophagic Machinery in Enterovirus Infection. *Viruses* 8: 32.

Lin K. & Gallay P. 2013. Curing a viral infection by targeting the host: the example of cyclophilin inhibitors. *Antiviral Res* 99: 68-77.

Lin J., Kung Y. & Shih S. 2019. Antivirals and vaccines for Enterovirus A71. *Journal of Biomedical Science* 26: 65.

Melia C.E., Peddie C.J., de Jong, Anja W. M., Snijder E.J., Collinson L.M., Koster A.J., van der Schaar, Hilde M., van Kuppeveld, Frank J. M. & Bárcena M. 2019. Origins of Enterovirus Replication Organelles Established by Whole-Cell Electron Microscopy. *mBio* 10: 951

Novak J.E. & Kirkegaard K. 1991. Improved method for detecting poliovirus negative strands used to demonstrate specificity of positive-strand encapsidation and the ratio of positive to negative strands in infected cells. *J. Virol* 65: 3384.

Ono Y. & Sorimachi H. 2012. Calpains: an elaborate proteolytic system. *Biochim Biophys Acta* 1824: 224-236.

Paul A.V. 2002. Possible Unifying Mechanism of Picornavirus Genome Replication. In: Semler B.L. & Wimmer E. (eds.), Molecular Biology of Picornavirus, American Society of Microbiology.

Pons-Salort M., Parker E.P.K. & Grassly N.C. 2015. The epidemiology of non-polio enteroviruses: recent advances and outstanding questions. *Curr Opin Infect Dis* 28: 479-487.

Roivainen M., Alfthan G., Jousilahti P., Kimpimaki M., Hovi T. & Tuomilehto J. 1998. Enterovirus Infections as a Possible Risk Factor for Myocardial Infarction. *Circulation* 98: 2534-2537.

Romero-Brey I. & Bartenschlager R. 2016. Endoplasmic Reticulum: The Favorite Intracellular Niche for Viral Replication and Assembly. *Viruses* 8: 160.

Rossmann M.G., He Y. & Kuhn R.J. 2002. Picornavirus–receptor interactions. *Trends in Microbiology* 10: 324-331.

Ruokolainen V., Domanska A., Laajala M., Pelliccia M., Butcher S. J., & Marjomäki V. 2019. Extracellular albumin and endosomal ions prime enterovirus particles for uncoating that can be prevented by fatty acid saturation. *Journal of Virology*, 93: 17, e00599-19.

Schindelin J., Arganda-Carreras I., Frise E., Kaynig V., Longair M., Pietzsch T., Preibisch S., Rueden C., Saalfeld S., Schmid B., Tinevez J., White D.J., Hartenstein V., Eliceiri K., Tomancak P. & Cardona A. 2012. Fiji: an open-source platform for biological-image analysis. *Nature Methods* 9: 676-682.

Tuthill T.J., Groppelli E., Hogle J.M. & Rowlands D.J. 2010. Picornaviruses. In: Johnson J.E. (ed.), Cell Entry by Non-Enveloped Viruses, Springer Berlin Heidelberg, Berlin, Heidelberg, pp. 43-89.

Upla P., Marjomäki V., Nissinen L., Nylund C., Waris M., Hyypiä T. & Heino J. 2008. Calpain 1 and 2 are required for RNA replication of echovirus 1. *J Virol* 82: 1581-1590.

van Buuren N. & Kirkegaard K. 2018. Detection and Differentiation of Multiple Viral RNAs Using Branched DNA FISH Coupled to Confocal Microscopy and Flow Cytometry. *Bio-protocol* 8: e3058.

van Der Schaar H.M., Dorobantu C.M., Albulescu L., Strating, J.R.P.M. & van Kuppeveld, F.J.M. 2016. Fat(al) attraction: Picornaviruses Usurp Lipid Transfer at Membrane Contact Sites to Create Replication Organelles. *Trends Microbiol* 24: 535-546.

Wang X., Lim H.J. & Son A. 2014. Characterization of denaturation and renaturation of DNA for DNA hybridization. *Environ Anal Health Toxicol* 29: 2014007.

Zhang Q., Xu L., Zhang Y., Wang T., Zou X., Zhu Y., Zhao Y., Li C., Chen K., Sun Y., Sun J., Zhao Q. & Wang Q. 2017. A novel ViewRNA in situ hybridization method for the detection of the dynamic distribution of Classical Swine Fever Virus RNA in PK15 cells. *Virology Journal* 14: 81.

APPENDIX 1. bDNA FISH protocol for detecting enterovirus RNA strands

Materials needed:

- ViewRNA Cell Plus Assay Kit
    - Fixation/Permeabilization Component A
    - Fixation/Permeabilization Component B
    - Blocking/Antibody Diluent
    - Solution A Fixative
    - Solution B Fixative
    - Probe Set Diluent
    - Amplifier Diluent
    - Label Probe Diluent
    - PBS (10X)
    - RNA Wash buffer component A
    - RNA Wash buffer component B
    - RNase Inhibitor (100X)
    - EVAB- and EVAB+ Probes
    - PreAmplifier Mix
    - Amplifier Mix
    - Label Probe Mix
- Round, autoclaved coverslips
- Microscopy glasses
- 4-well plates
- Sterile glass petri dishes
- A scalpel and/or tweezers
- Cells and viruses
- DMEM (1% and 10%)
- Ice-cold 0,5% BSA-PBS
- Nuclease free water
- 95% Formamide in 0,1% SSC Buffer

- Primary antibody(s)
- Secondary antibody(s)
- DAPI diluted 1:40 000 in 1X PBS
- Mowiol-DABCO

Day 1: Preparing cells for the experiment

1. Prepare as many coverslips on 5 ml plate(s) for your cells as you need (+ maybe a few extra) by putting sterile round coverslip on the bottom of a 5 ml plate, max 10 per plate
2. Split your cells as per usual
3. If you had a 90-100% confluent T75 bottle, use a 1:5 or 1:6 dilution for the 5 ml plate (this way the 5 ml plate with the coverslips will be 70-80% confluent the next day)
4. Add media to the 5 ml plate so that the total volume is around 5 ml
5. Incubate in 37 °C overnight.

Day 2: Infections, fixing and permeabilization

6. Mark 4-well plates for your samples (1 well per sample). Add 500 µl of PBS to the wells.
7. Move coverslips from the 5 ml plate to the 4-well plates (1 coverslip per well) using a clean scalpel or tweezers, cells facing up.
8. Prepare your virus dilution: 1:3000 in 1% DMEM for CVA9, CVB3 and EV1 is fine. Prepare at least **200 µl per well**. Mix well.
9. Fill a styrox box with ice and cover it with a metal plate: take it to the laminar and put your 4-well plates on the cold metal plate.
10. Aspirate PBS from wells, add 200 µl of diluted virus.
11. Put the box on a rocker, incubate for 45 minutes (ice-binding of the virus).
12. Aspirate the virus solution
13. Wash 3 x 5 minutes with 0,5% ice-cold BSA-PBS
14. Add 400 µl of 10% DMEM to the wells
15. Incubate at 37°C for as long as you need to (e.g. 5h).

16. Prepare Fixation/Permeabilization Solution for all samples by combining **110 µl** of Fixation/Permeabilization Component A with **110 µl** of Fixation/Permeabilization Component B **per sample. Mix well.**
17. Prepare 1X PBS with RNase Inhibitor (**1 ml per sample**) by diluting the 100X RNase Inhibitor and the 10X PBS in nuclease free water. Mix well.
18. After the virus incubation, aspirate the 10% DMEM.
19. Add **200 µl** of Fixation/Permeabilization Solution per well
20. Incubate for 30 minutes at room temperature on the rocker
21. Aspirate the Fixation/Permeabilization solution
22. Wash three times with the 1X PBS with RNase Inhibitor, **300 µl per well per wash**
23. **Be gentle with the washing; you can prepare additional wash buffer and use a dropper to wash the wells gently if you want to. There is no need to incubate the cells in the wash buffer between washes.**
24. Leave the cells in the 1X PBS with RNase inhibitor
25. Seal the edges of the plates with parafilm, store at +4°C overnight.

Day 3: Antibody staining and target probe hybridization

26. Prepare Blocking/Antibody Diluent Solution (**550 µl per sample**) by diluting RNase inhibitor (100X) to a 1:100 dilution with Blocking/ Antibody Diluent.
27. Aspirate the 1X PBS with RNase inhibitor from the wells
28. Add **200 µl** of Blocking/Antibody Diluent Solution per well
29. Incubate for 20 minutes at room temperature on the rocker
30. Dilute primary antibodies in Blocking/Antibody Diluent Solution **(155 µl per sample).**
31. Dilute secondary antibodies in Blocking/Antibody Diluent Solution **(155 µl per sample)**
32. Aspirate Blocking/Antibody Diluent Solution from the wells
33. Add **150 µl** of primary antibody solution per well
34. Incubate for 1 hour at room temperature on the rocker

35. Prepare 1X PBS with RNase inhibitor as in step 17., **3 ml per sample**.
36. Aspirate the primary antibody solution
37. Wash three times with the 1X PBS with RNase Inhibitor, **300 µl per well per wash**
38. Add **150 µl** of secondary antibody solution per well
39. Incubate for 30 minutes at room temperature on the rocker
40. Aspirate the secondary antibody solution
41. Wash three times with the 1X PBS with RNase Inhibitor, **300 µl per well per wash**
42. Prepare Fixation solution by combining **27,5 µl** of Solution A Fixative with **192,5 µl** of Solution B Fixative **per sample. Mix well.**
43. Add **200 µl** of Fixation solution per well
44. Incubate for 1 hour at room temperature on the rocker
45. During the incubation:
    a. Thaw the target probes (e.g. EVAB- and EVAB+) and maintain on ice
    b. Pre-warm Probe Set Diluent to 40°C
    c. Prepare Wash Buffer Solution by combining **1587,2 µl** of nuclease-free water, **4,8 µl** of Wash Component 1 and **8 µl** of Wash Component 2 **per sample. Mix well.**
    d. Take a heating block to a fume hood and warm it to 65 °C.
    e. Mark spots on the bottom of a sterile glass petri dish for your samples so you don't confuse the samples.
46. Aspirate the Fixation Solution
47. Wash three times with the 1X PBS with RNase Inhibitor, **300 µl per well per wash**
48. Maintain the coverslips in PBS on the 4-well plates and take the plates to the fume hood
49. Add 95% formamide in 0,1X SSC Buffer to the glass dishes (around 5 ml)
50. Transfer the coverslips to the glass dishes and leave the PBS in the 4-well plates
51. Place the glass dishes on top of the heating block in the fume hood

52. Incubate for 15 minutes on top of the 65°C heater block
53. Transfer the coverslips back to the 4-well plates with PBS in the wells
54. Wash quickly once with 1X PBS with RNase Inhibitor, **300 µl per wash**
55. Dilute the Probe Set(s) 1:100 in the pre-warmed Probe Set Diluent. If using more than one probe, dilute them into the same solution. Prepare **155 µl per sample and mix well.**
56. Aspirate the 1X PBS with RNase inhibitor.
57. Add **150 µl** of the Diluted Target Probe per well
58. Incubate for 2 hours at 40°C incubator
59. Aspirate the Diluted Target Probe
60. Wash five times with the Wash Buffer prepared in step 45c, **300 µl per wash per well**
61. Leave the cells in the Wash Buffer
62. Seal the edges of the plates with parafilm, store at +4°C overnight.

Note: Formamide keeps the RNA strands separated for only 10-15 minutes, so you have to be quick between taking the cells out from the formamide and adding the Target Probe Set.

Day 4-5: Signal amplification and confocal microscopy

63. Pre-warm the samples to room temperature
64. Pre-warm Amplifier Diluent and Label Probe Diluent to 40°C
65. Thaw PreAmplifier Mix, Amplifier Mix and Label Probe Mix and maintain on ice
66. Prepare Wash Buffer Solution by combining **4761,6 µl** of nuclease-free water, **14,4 µl** of Wash Component 1 and **24 µl** of Wash Component 2 **per sample. Mix well.**
67. Prepare the PreAmplifier Solution by diluting the PreAmplifier Mix 1:25 in the Amplifier Diluent. Prepare **155 µl per sample and mix well.**
68. Aspirate the Wash Buffer from the wells
69. Add **150 µl** of the PreAmplifier Solution per well
70. Incubate for 1 hour at 40°C

71. Aspirate the PreAmplifier Solution
72. Wash five times with the Wash buffer, **300 µl per wash per well**
73. Prepare the Amplifier Solution by diluting the Amplifier Mix 1:25 in the Amplifier Diluent. Prepare **155 µl per sample and mix well.**
74. Aspirate the Wash Buffer from the wells
75. Add **150 µl** of the Amplifier Solution per well
76. Incubate for 1 hour at 40°C
77. Aspirate the Amplifier Solution
78. Wash five times with the Wash buffer, **300 µl per wash per well**
79. Prepare the Label Probe Solution by diluting the Label Probe Mix 1:25 in the Amplifier Diluent. Prepare **155 µl per sample and mix well.**
80. Aspirate the Wash Buffer from the wells
81. Add **150 µl** of the Label Probe Solution per well
82. Incubate for 1 hour at 40°C
83. Aspirate the Label Probe Solution
84. Wash five times with the Wash buffer, **300 µl per wash per well**
85. Let the coverslips incubate in the final wash for 10 minutes at room temperature
86. Wash once with normal 1X PBS (no RNase inhibitors needed), **300 ul per well**
87. Add **150 µl** of DAPI diluted 1:40 000 in 1X PBS per well
88. Incubate for 5 minutes at room temperature on the rocker
89. Wash once with 1X PBS
90. Mark microscopy glasses well with a pencil
91. Add 10 µl of Mowiol-DABCO per coverslip on the glass (1-2 coverslips per glass)
92. Mount the coverslips on the glass, **cells facing downwards.**
93. Let dry overnight at +4°C
94. Visualize with confocal microscope.